Impacts of Varying Model Physics on Simulated Structures in Cloud Systems

Andrew Lesage
PhD Candidate, Department of Atmospheric Sciences
University of Utah
18 August, 2017

Outline

Introduction

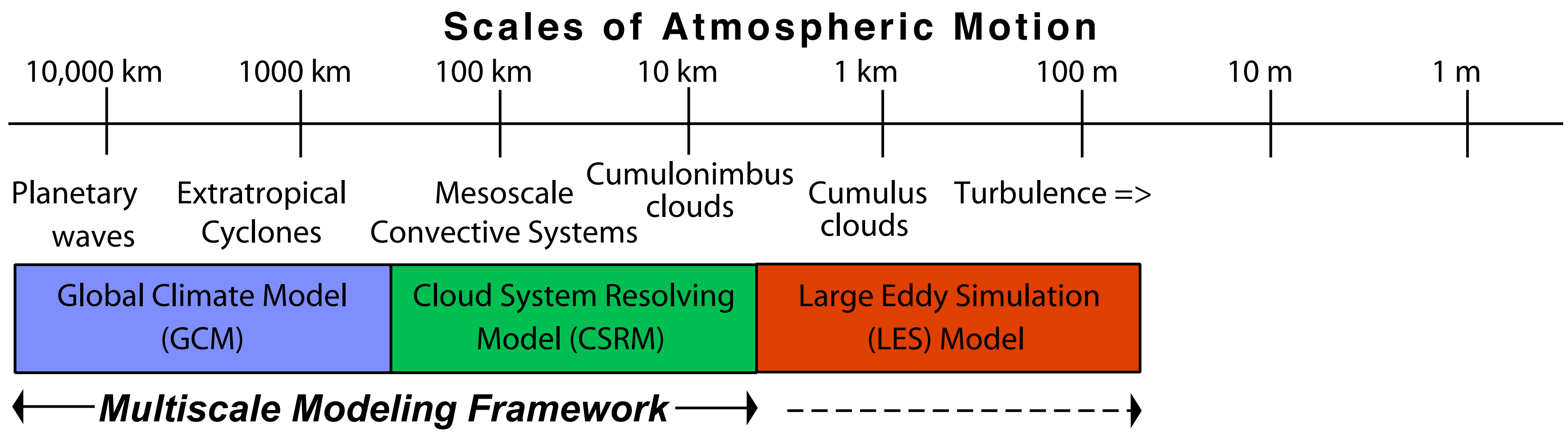

Boundary layer clouds and turbulence occur on small enough scales that they are unable to be resolved in global climate models (GCMs).

Turbulence parameterization schemes have been essential in GCMs and cloud resolving models (CRMs) to represent sub-grid scale (SGS) processes.

In large-eddy simulation (LES) models large eddies and shallow convection are resolved, while smallest eddies are parameterized.

100m SHDOM image made by Ian Glenn

Introduction

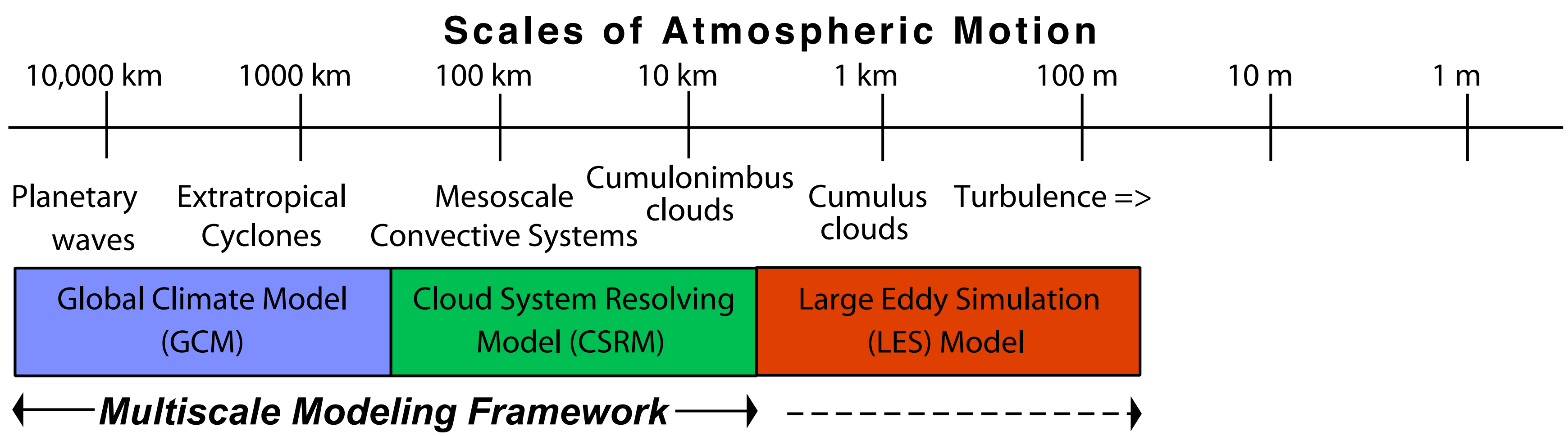

- Grey Zone - NWP grid size range between ~1 km and ~10 km where the model grid size is approximately that of individual clouds.

- The grey zone is a transition range where features become more resolved though parameterization is still essential.

Simplified Higher-Order Closure (SHOC)

-SHOC (Bogenschutz and Krueger, 2013) is a turbulence closure scheme which:

- prognoses SGS-TKE
- uses an assumed joint PDF to diagnose SGS condensation and buoyancy (Golaz et al., 2002a,b)
- uses vertical velocity, liquid water potential temperature, and total water mixing ratio for a double Gaussian joint PDF which more accurately represents skewness (Bogenschutz et al., 2010).
- uses the diagnostic second-moment closure of Redelsperger and Sommeria (1986) and the third-moment closure of vertical velocity from Canuto et al. (2001).

System for Atmospheric Modeling (SAM)

-Used throughout as both a Large-Eddy Simulation (LES) for 100 m runs and as a Cloud-Resolving Model (CRM) for larger grid spacings. Detailed in Khairoutdinov and Randall (2003).

-Uses anelastic equations of motion in the dynamical core.

-Prognoses thermodynamical variables: 1. liquid water/ice moist static energy, 2. total non-precipitating water, 3. total precipitating water.

-Periodic boundary conditions.

-Monin-Obukhov similarity theory for surface fluxes.

System for Atmospheric Modeling (SAM)

-Radiation uses either:
1. the Community Atmospheric Model (CAM, Collins and Coauthors, 2004)
or
2. the Rapid Radiative Transfer Model (RRTM, Mlawar et al., 1997).

-Microphysics uses either:
1. SAM single-moment (Khairoutdinov and Kogan, 2000)
or
2. Morrison double-moment (Morrison et al., 2005).

SAM-TKE (NOSHOC)

-SAM turbulence closure scheme options include a 1.5-order closure using a prognostic subgrid-scale turbulent kinetic energy (SGS-TKE) equation (Khairoutdinov and Kogan, 1999), a simple Smagorinsky closure (Khairoutdinov and Randall, 2003), and SHOC.

-The first of which is used throughout this research as "NOSHOC".

-NOSHOC does not diagnose SGS condensation and uses the moist Brunt-Vaisala frequency to diagnose SGS buoyancy.

-NOSHOC uses the "all-or-nothing" approach for cloud condensate and cloud fraction.

SHOC vs NOSHOC

-A key difference between NOSHOC and SHOC is in the handling of the turbulence length scale.

-NOSHOC: length scale proportional to dz, appropriate for high resolution simulations (Bogenschutz and Krueger, 2013)

-SHOC: length scale is related to SGS-TKE and eddy length scales (Teixeria and Cheinet, 2004; Cheng et al., 2010)

CONSTRAIN - Background

- Marine cold air outbreak - a polar air mass being advected into an area with warmer water (Brümmer, 1996).
- Convection morphs from organized rolls to open cells (Brümmer, 1999).
- Marine cold air outbreaks are more common in SH but stronger in NH (Fletcher et al., 2016a).
- Generally low level clouds and a high cloud fraction (Fletcher et al., 2016b).
- Common for mixed-phase clouds with supercooled liquid clouds precipitating ice (Hobbs and Rangno, 1998).

CONSTRAIN - Background

Cold air outbreak examples (a, continental, b, marine).

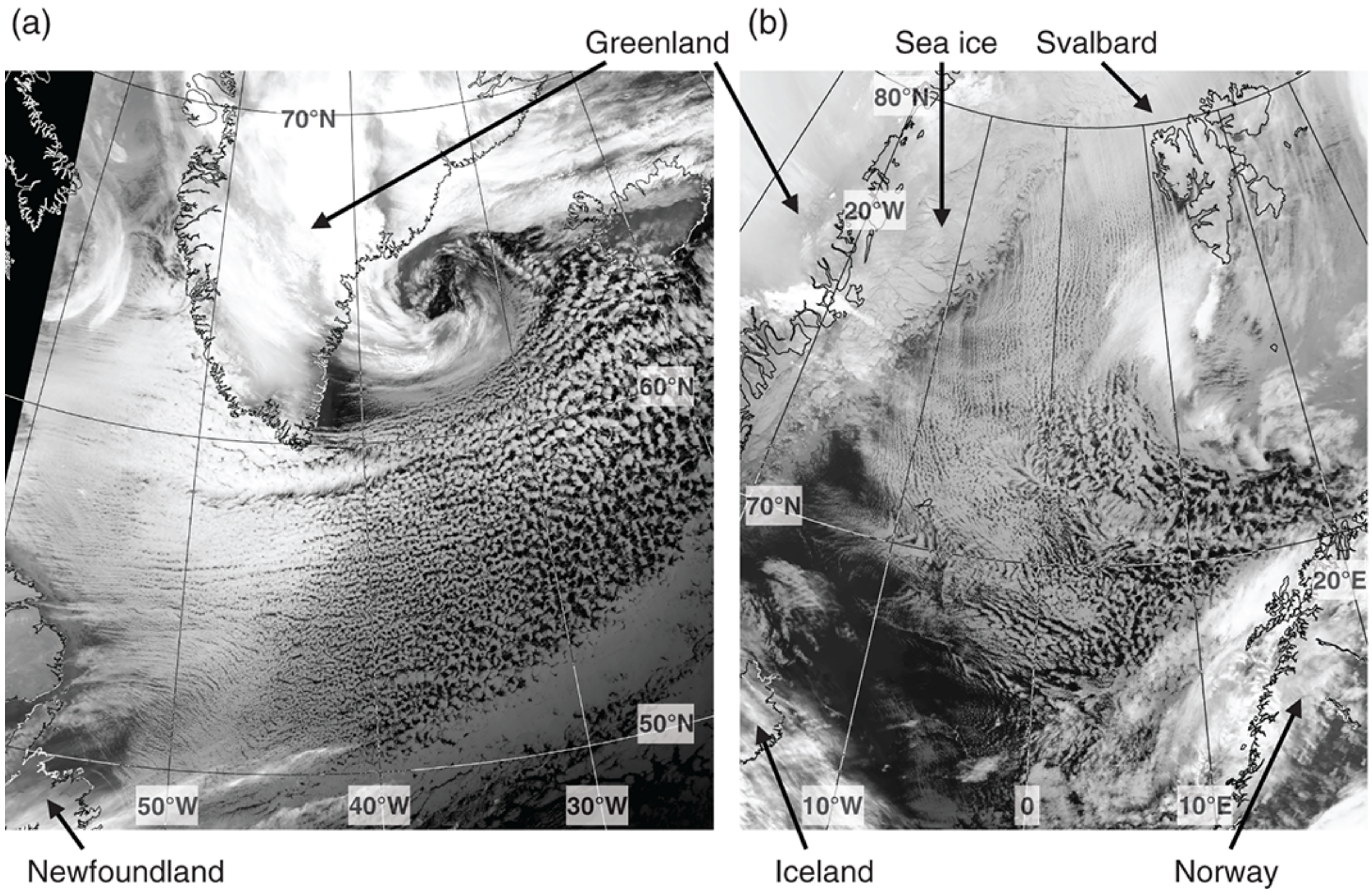

Figure 1 of Kolstad (2017)

CONSTRAIN - Background

CONSTRAIN details:

-Met Office field campaign over the Northern Atlantic Ocean

-Cold air outbreak event, 31 January 2010.

-14.5 hour long case, first 1.5 hrs are spin-up.

-Initial conditions and forcing generated from high resolution limited area model simulation (Field et al., 2014).

-Quasi-lagrangian model simulates transition from Sc to Cu (66°N 11°W to 60°N 8.7°W).

-SST (increase) forcing applied through simulation.

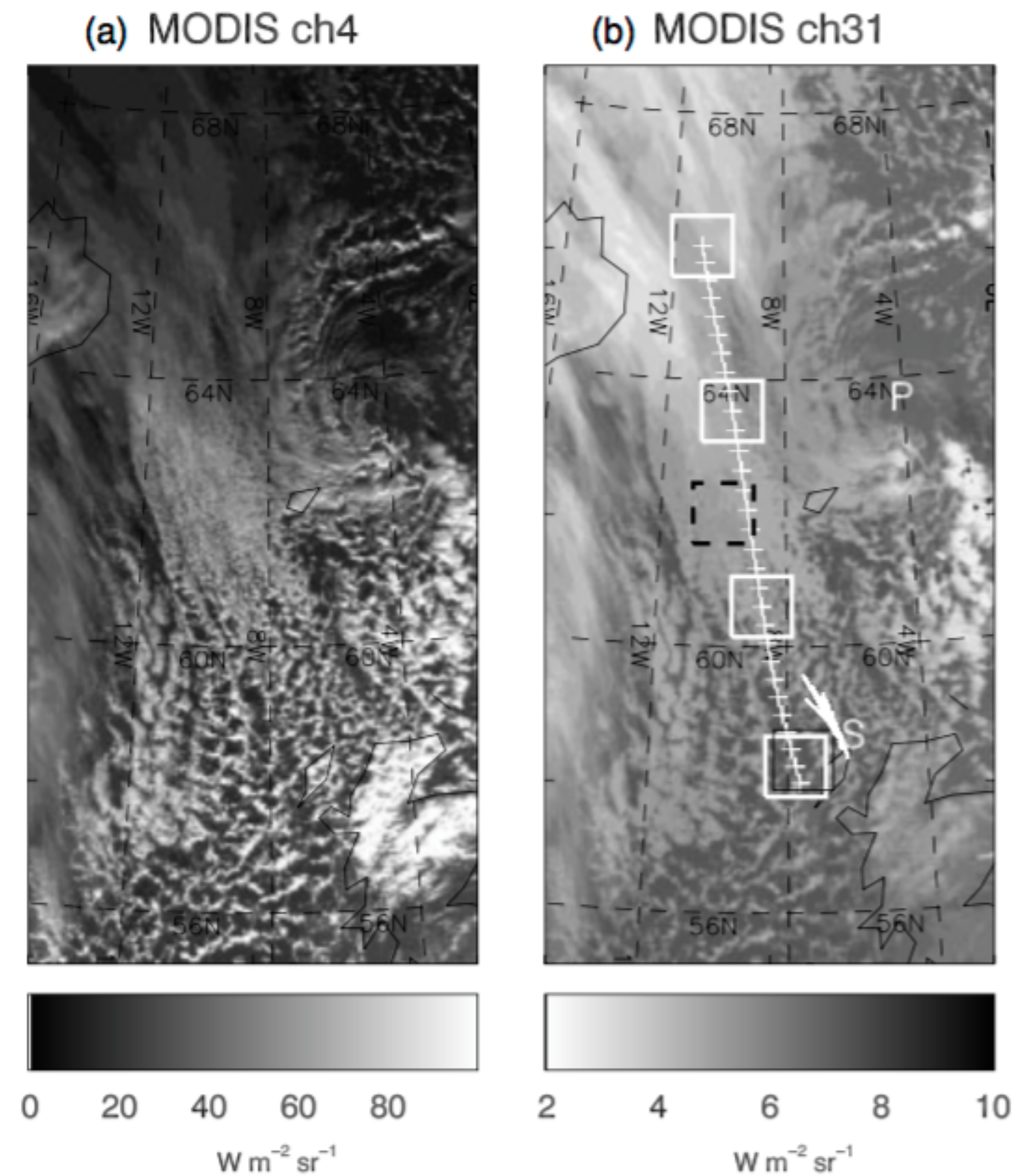

Figure 2a,b of Field et al. (2014)

CONSTRAIN
- Model Runs

	NOSHOC				
Grid Spacing	30 km	3 km	1 km	.5 km	.1 km
Full Physics	x	x	x	x	x
No Precipitation					x
No Rad.	x	x	x	x	x
No Rad./Prec.					x
No Ice		x	x	x	x
Ice Only					x
Ice Only, No Sed.					x
No Sed.					x
Ice Only, No Rad/Sed./Prec.					x
No Cloud/Rad./Prec.					x
No Ice/Rad./Prec.					x
M2005		x			x

	SHOC					
Grid Spacing	30 km	8 km	4 km	3 km	1 km	.5 km
Full Physics	x			x	x	x
No Precipitation					x	x
No Rad.	x			x	x	x
No Rad./Prec.						
No Ice	x	x		x	x	x
Ice Only	x			x	x	x
No Sed.				x	x	x
Ice Only, No Rad/Sed./Prec.		x	x		x	
M2005				x		

CONSTRAIN - LES Results

What impact does radiation and precipitation have on clouds?

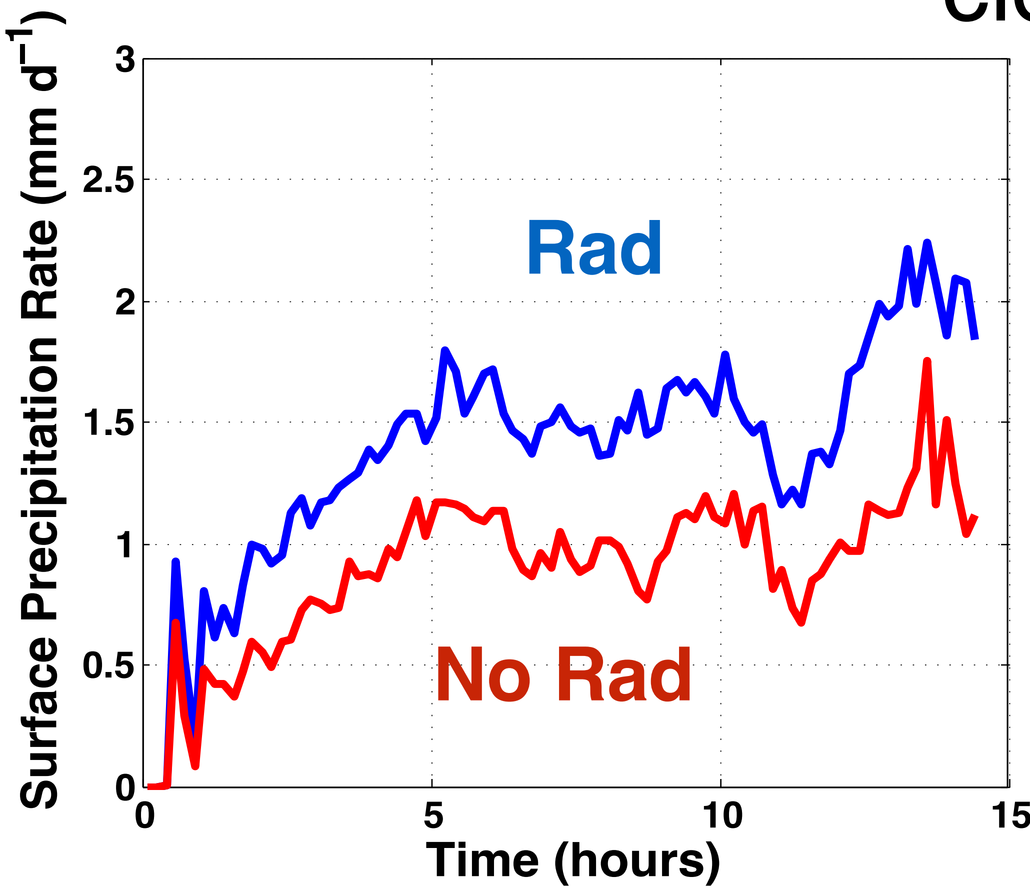

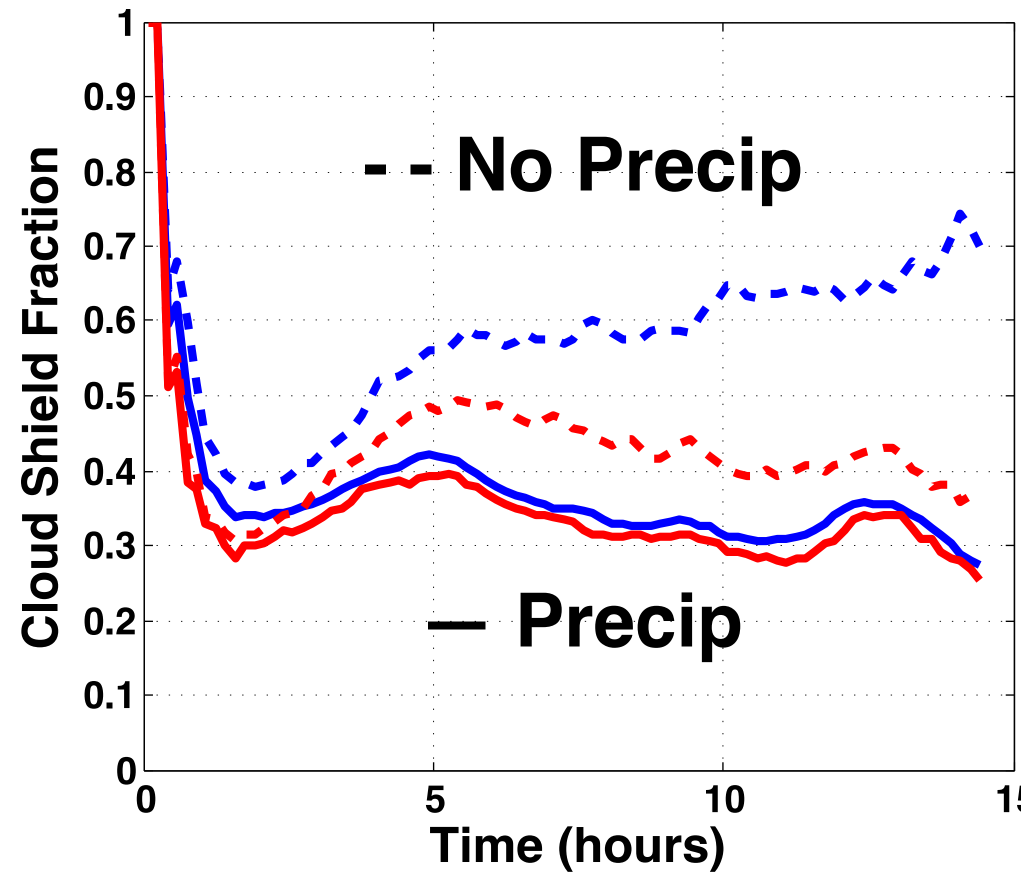

The radiation-allowing run (solid blue) had ~50% more precipitation but only marginally more cloud cover. Why?

In runs without precipitation radiation increases cloud cover (blue dashed vs red dashed).

Allowing precipitation (solid vs dashed) reduces cloud cover.

CONSTRAIN - LES Results

What influence does ice sedimentation have on clouds and entrainment?

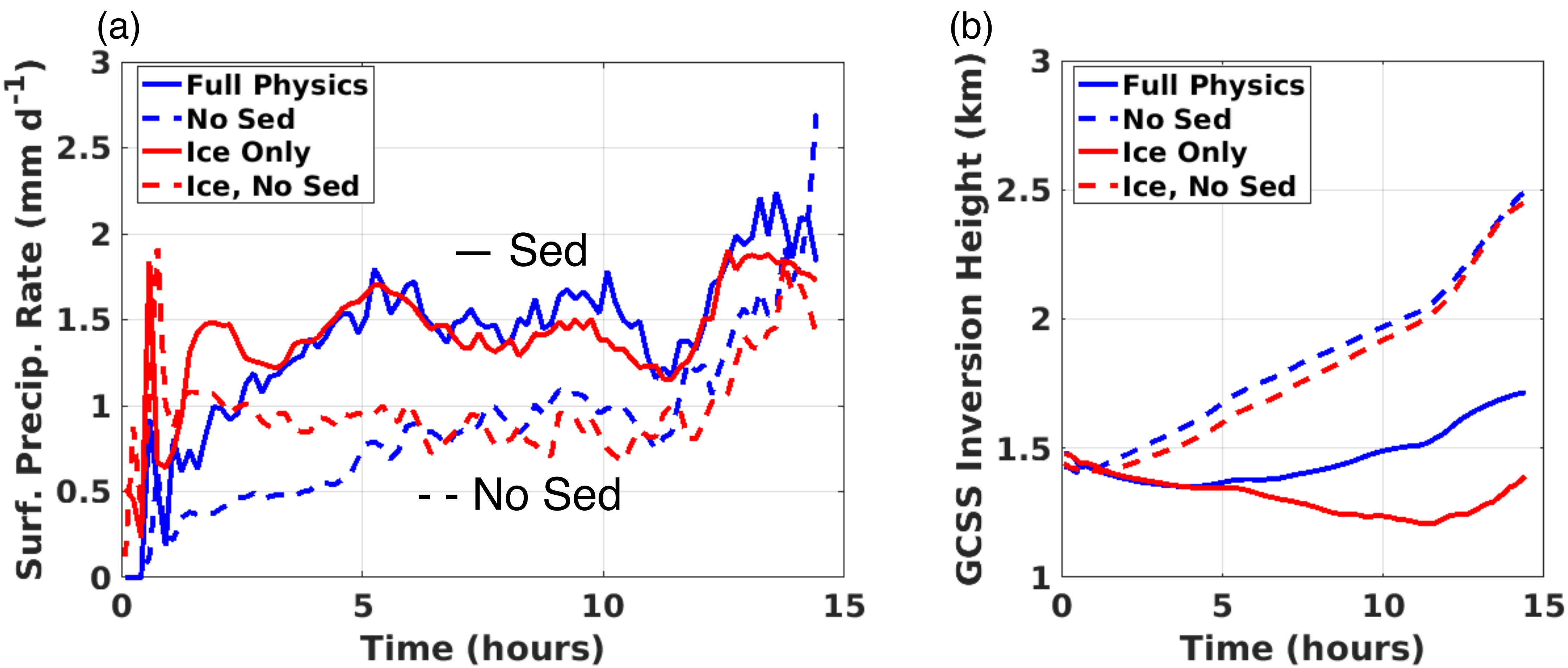

Runs without ice sedimentation have lower precipitation rates and higher inversion heights.

CONSTRAIN - LES Results

What influence does ice sedimentation have on clouds and entrainment?

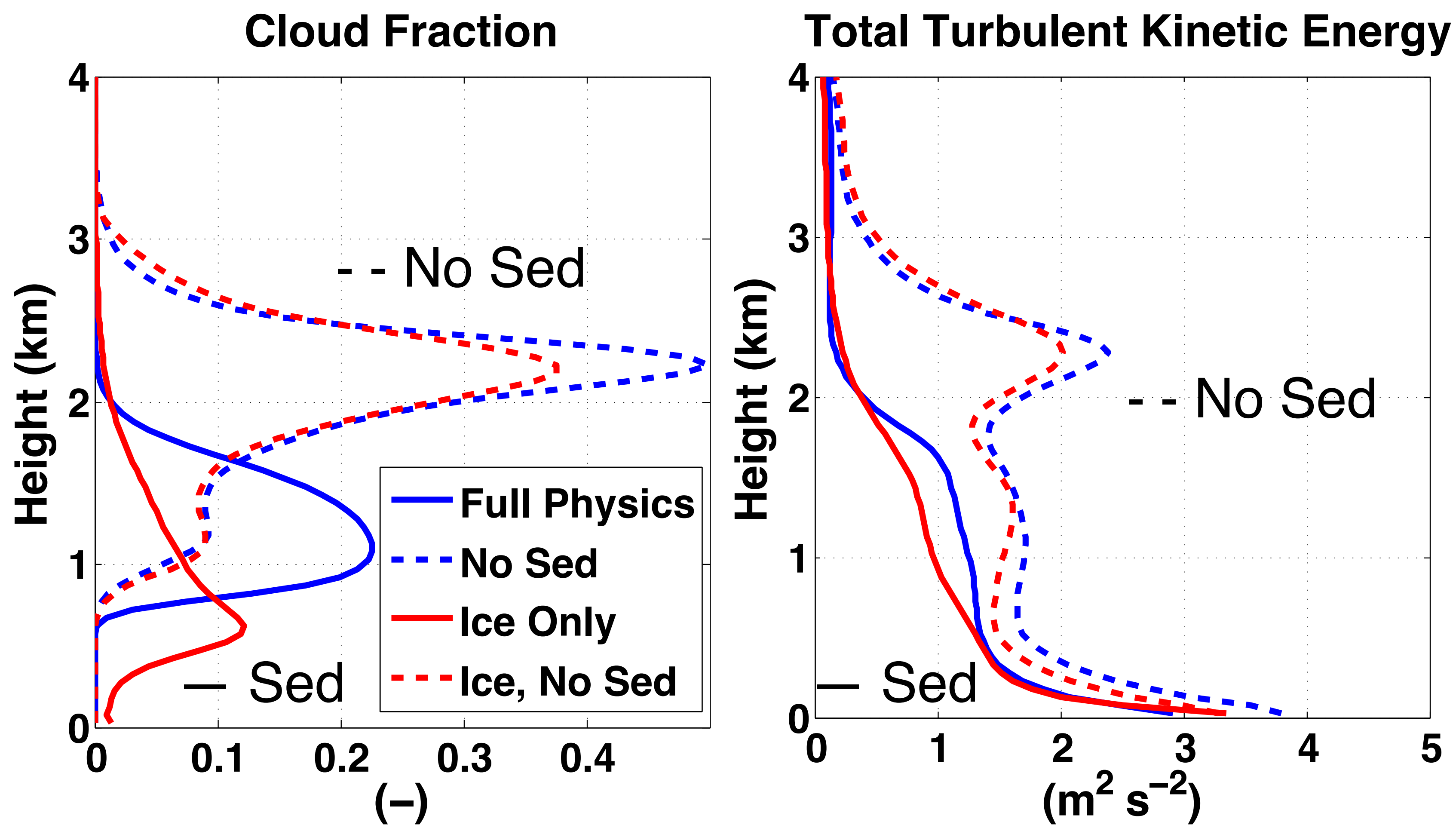

Runs without ice sedimentation have higher cloud fractions, higher TKE, and higher entrainment.

CONSTRAIN - LES Results

Does microphysics scheme matter? How about ice?

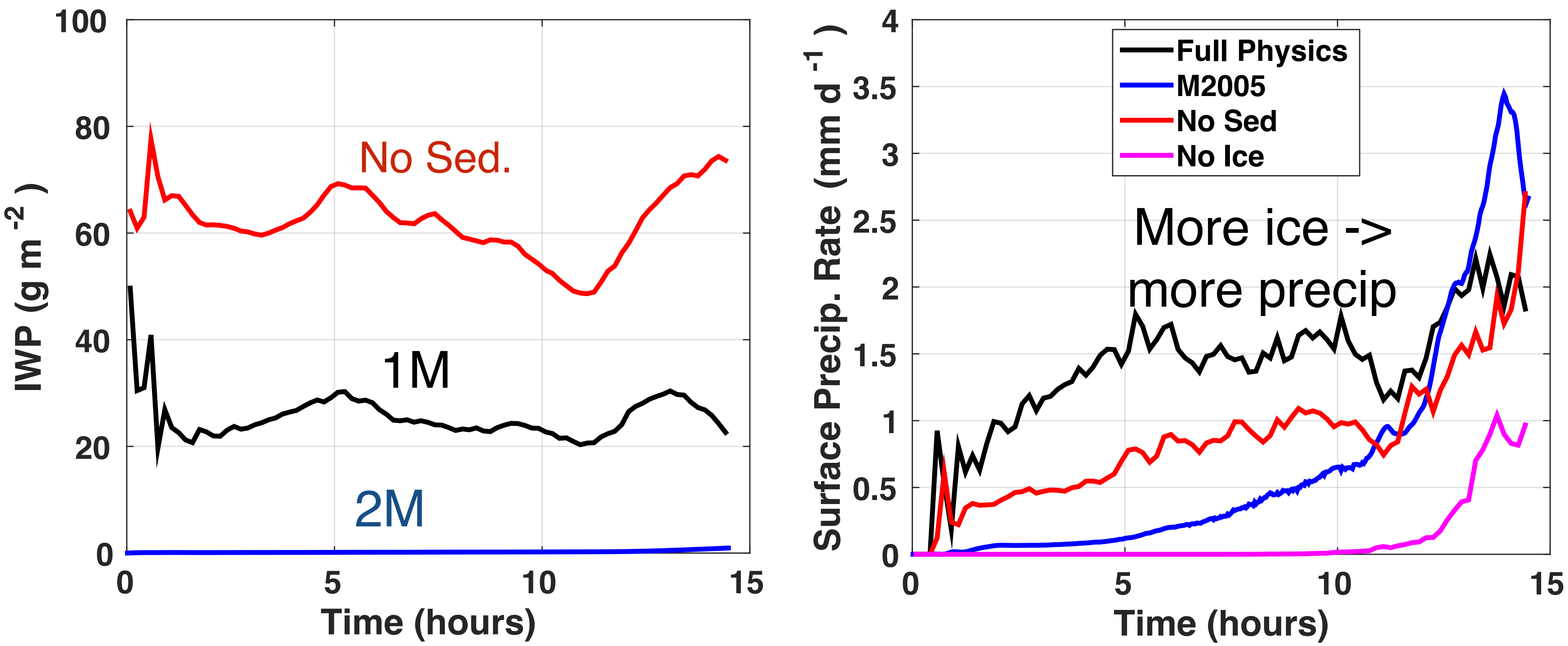

Much more ice in single moment (full physics) than double moment (M2005). M2005 has supercooled liquid water instead.

Similar result to other studies (Morrison and Pinto, 2006; Klein et al., 2009).

More precipitation in runs with ice.

CONSTRAIN - LES Results

Does microphysics scheme matter? How about ice?

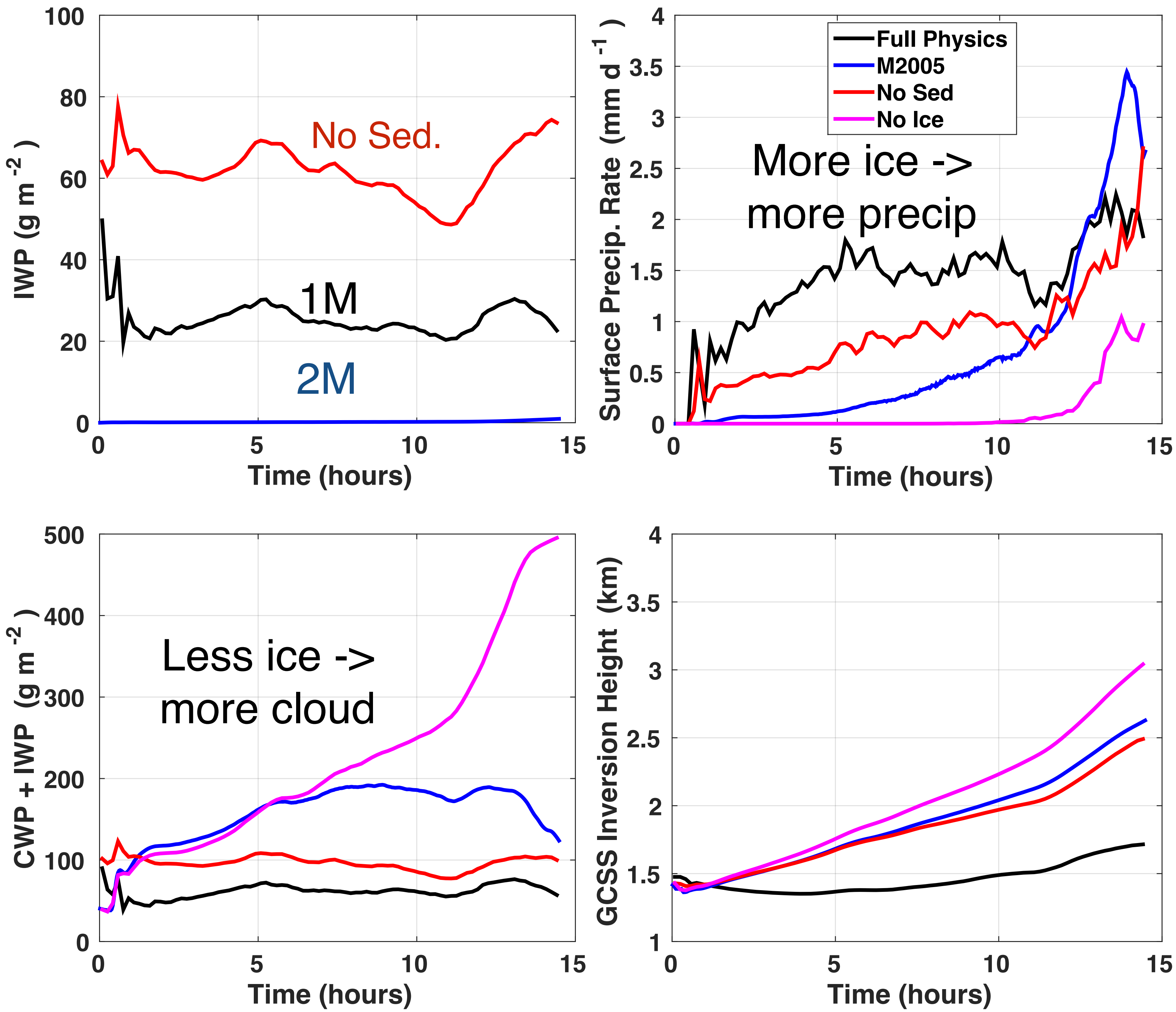

More cloud and entrainment in runs without ice.

CONSTRAIN Summary

- Radiation -> increasing cloud cover. Precipitation -> decreasing cloud cover.

- Ice sedimentation -> fewer clouds and less entrainment.

- Double-moment microphysics produces supercooled water instead of ice.

- Runs without ice produce more cloud.

RCE Background

Radiative convective equilibrium (RCE) runs are a simple proxy for the Earth.

RCE is a balance between radiative cooling of the atmosphere and heating from convection.

Have long been used for climate sensitivity studies (Manabe and Wetherald, 1964).

Clouds (and aerosols) feedbacks are the largest sources of uncertainty in climate models (Cess et al., 1996; Myhre et al., 2013).

Radiation budgets can be looked at with cloud bins sorted by optical thickness and elevation (Hartmann et al., 2001).

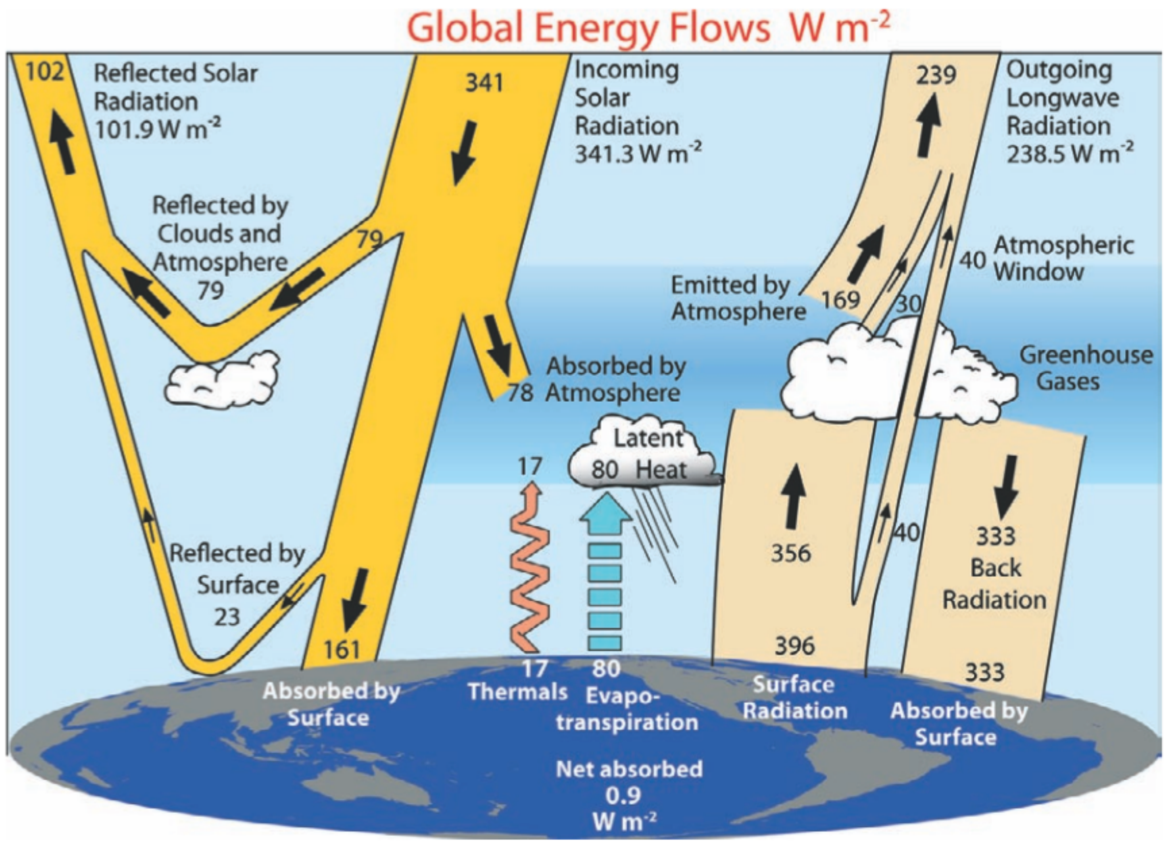

Fig. 1. The global annual mean Earth's energy budget for the Mar 2000 to May 2004 period ($W m^{-2}$). The broad arrows indicate the schematic flow of energy in proportion to their importance.

Trenberth et al. (2009)

RCE Model Runs

RCE simulations were performed to test cloud and radiative property dependence on many configurations:
-grid spacing
-turbulence parameterization scheme
-microphysics scheme
-SST, to evaluate cloud radiative feedbacks

Runs were performed for 50 day simulations, all results shown later are latter 25 day averages.

Runs were originally performed on 256 km x 256 km domains with 84 vertical levels. Some runs self-aggregated, necessitating smaller domains (Bretherton et al., 2005).

Aggregation has been shown to be dependent on the parameterization of SGS mixing (Tompkins and Semie, 2017).

RCE Model Runs

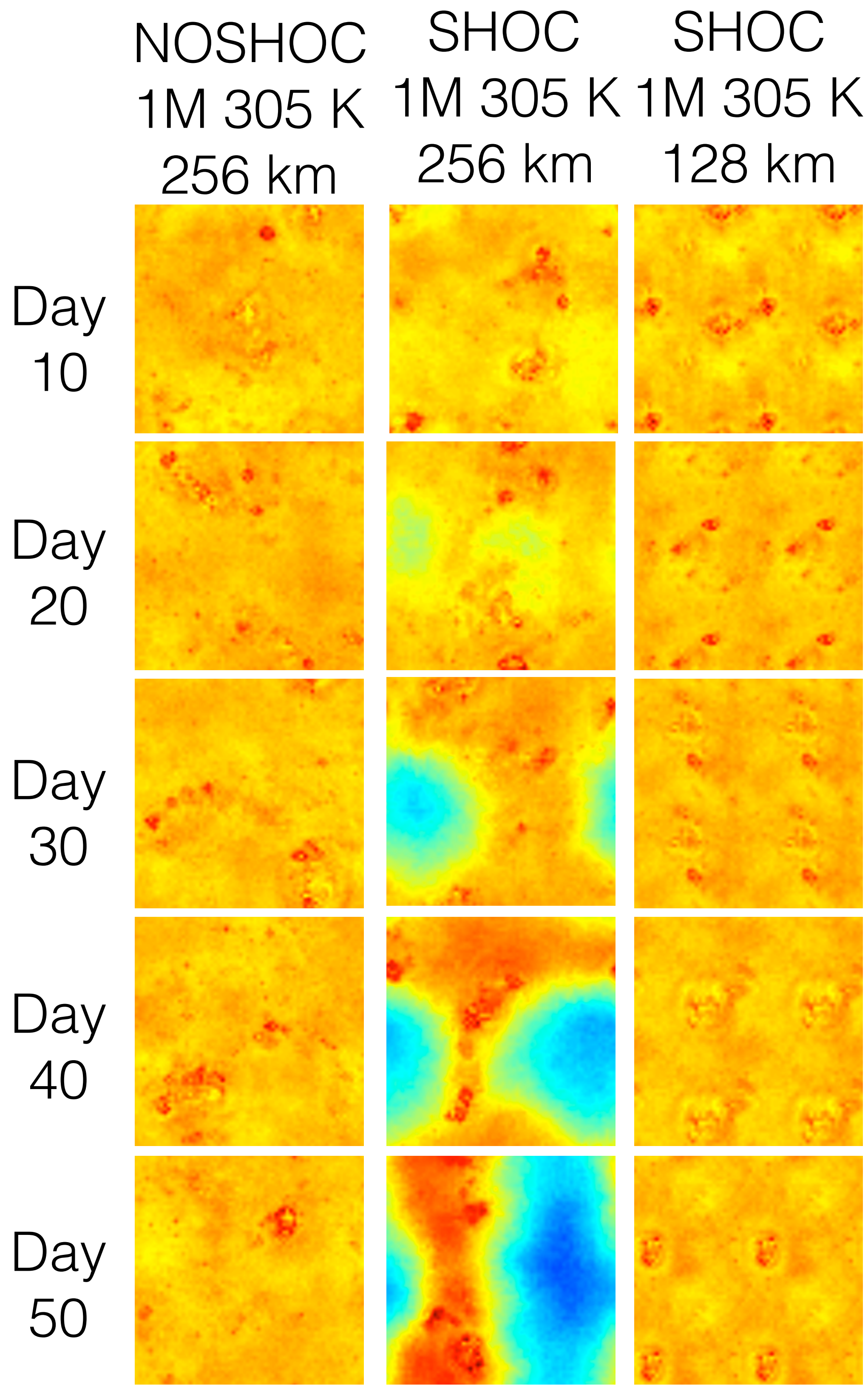

Example PW fields of an aggregating run vs a non-aggregating run.

RCE Model Runs

	NOSHOC 1M 305 K 256 km	SHOC 1M 305 K 256 km	SHOC 1M 305 K 128 km

Day 10

Day 20

Day 30

Day 40

Day 50

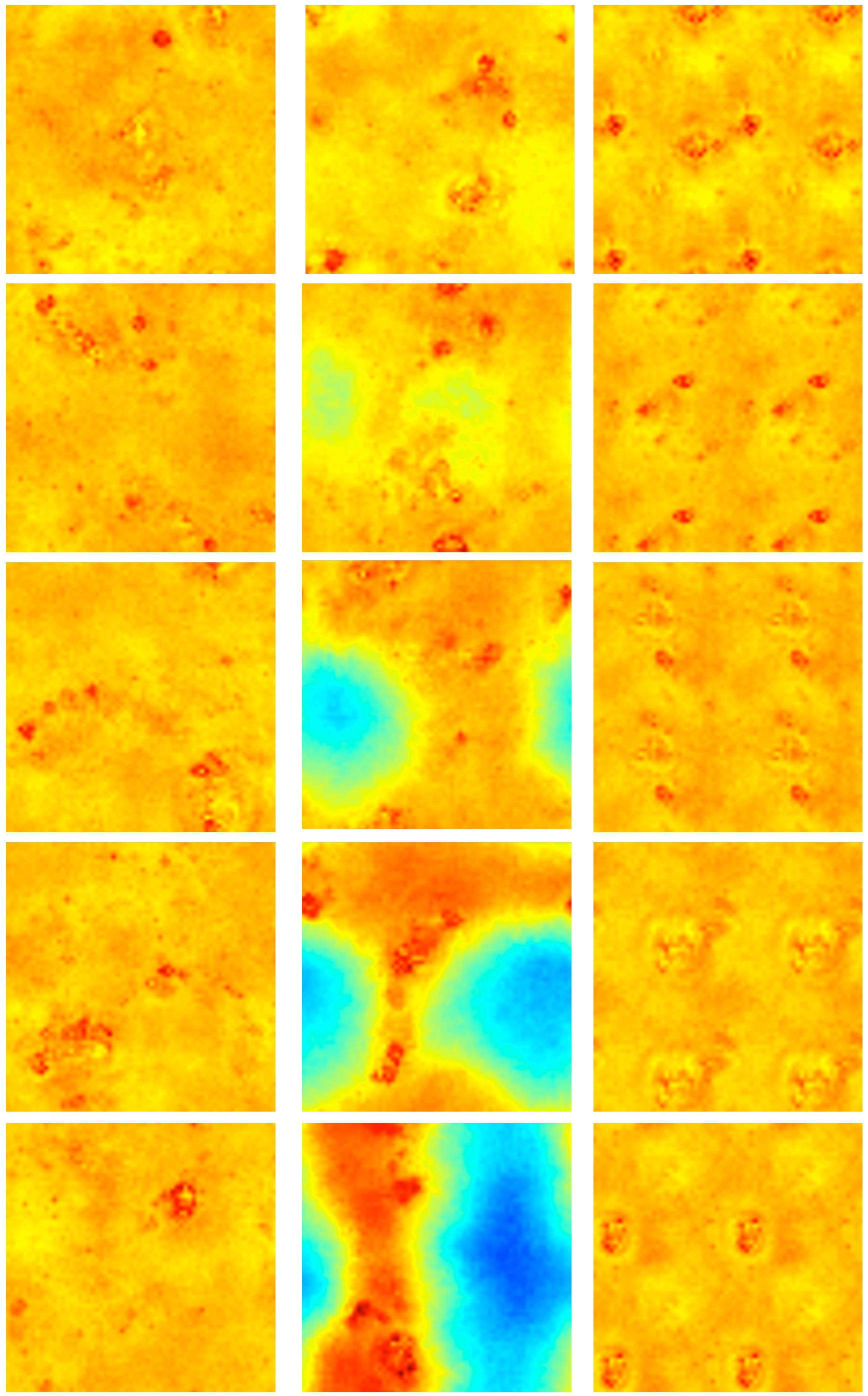

If your PW field starts to look like Grand Prismatic…

… it's self-aggregating.

https://www.yellowstonepark.com/things-to-do/grand-prismatic-midway-geyser-basin Grand Prismatic Hot Spring in Yellowstone. Photo by Grant Ordelheide

RCE Model Runs

TABLE 2. Model simulations performed for the RCE case.

RCE Run Setup			Grid Spacing (km)					
SST	Microphys.	Turb.	16	8	4	2	1	0.5
301 K	1M	NOSHOC	256	256	256	256	256	256
		SHOC	128	128	128	128	128	N/A
	2M	NOSHOC	256	256	256	256	256	N/A
		SHOC	128	128	64	64	64	N/A
305 K	1M	NOSHOC	256	256	256	256	256	256
		SHOC	128	128	128	256	256	N/A
	2M	NOSHOC	256	256	256	256	256	N/A
		SHOC	128	128	64	64	64	N/A
			Domain Size (km)					

Grid spacing: 16, 8, 4, 2, 1, 0.5 km.

Turbulence scheme: NOSHOC, SHOC

SSTs: 301 K, 305 K

Microphysics: single-moment, double-moment

Domain size: 256, 128, 64 km.

RCE Results: CWP & IWP

Single moment

Double moment

All results from final 25-day averages.

Higher CWP in double-moment runs.

IWP

CWP

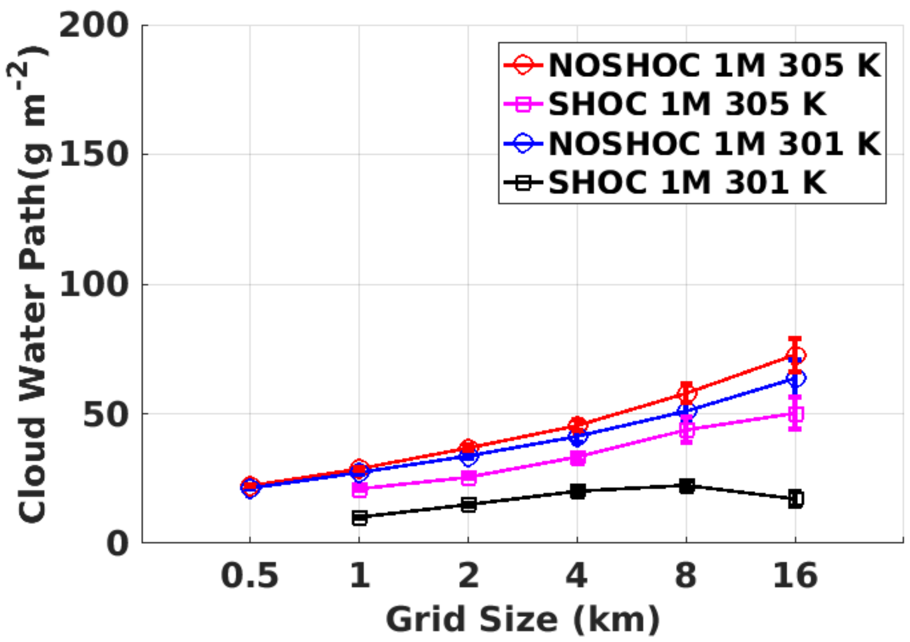

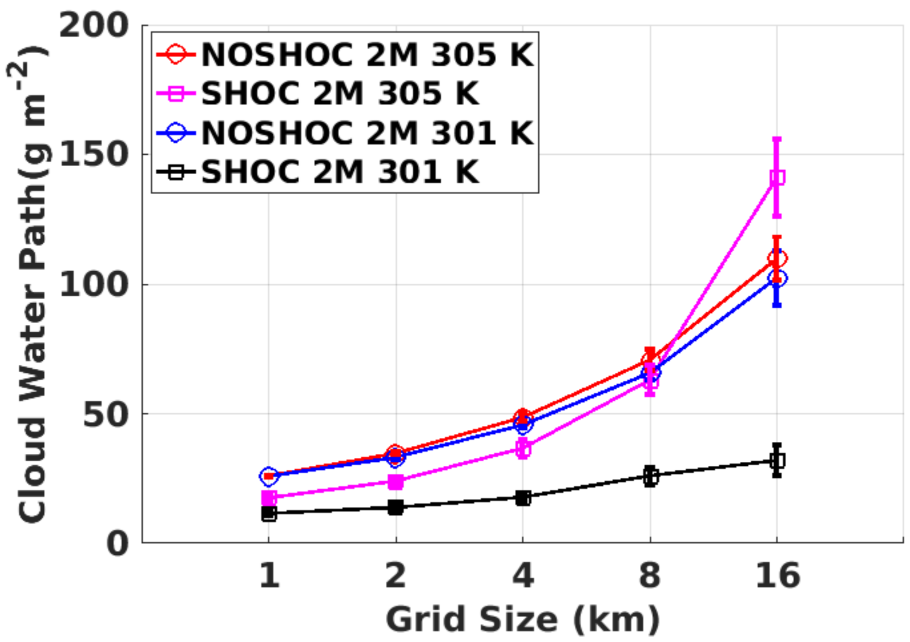

RCE Results: CWP & IWP

All results from final 25-day averages.

Single moment

Double moment

IWP

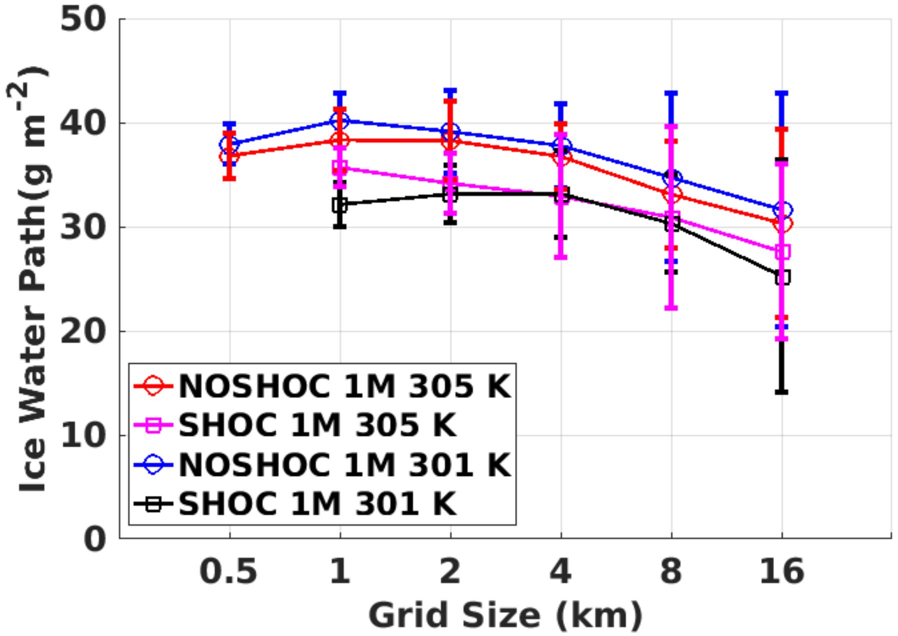

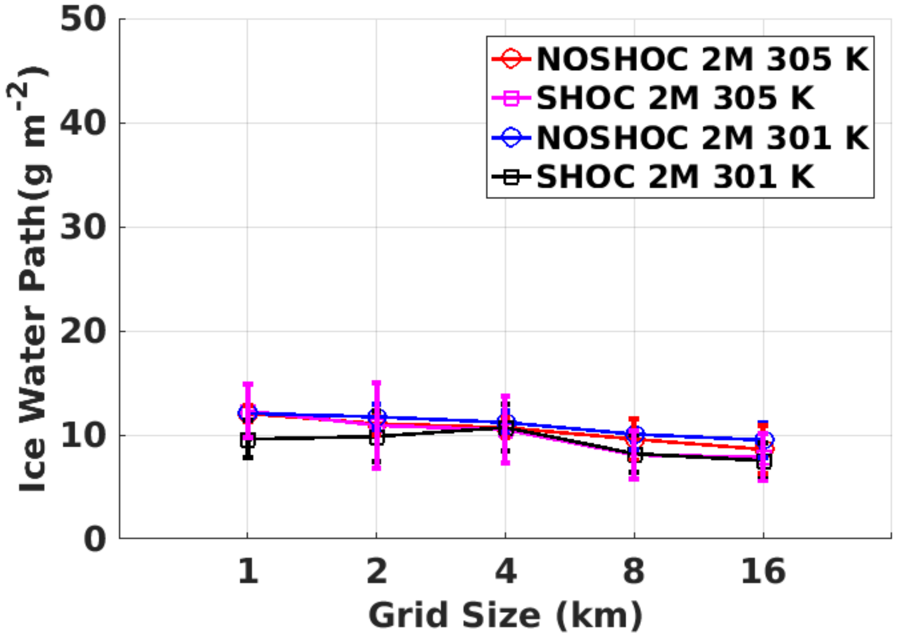

Lower IWP in double-moment runs.

CWP

RCE Results: CWP & IWP

Single moment

Double moment

IWP

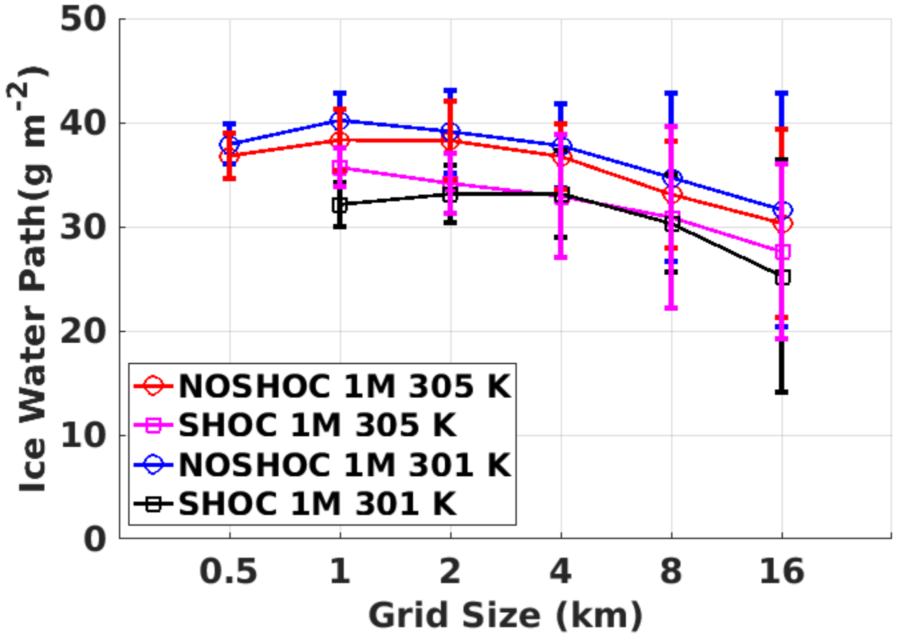

CWP

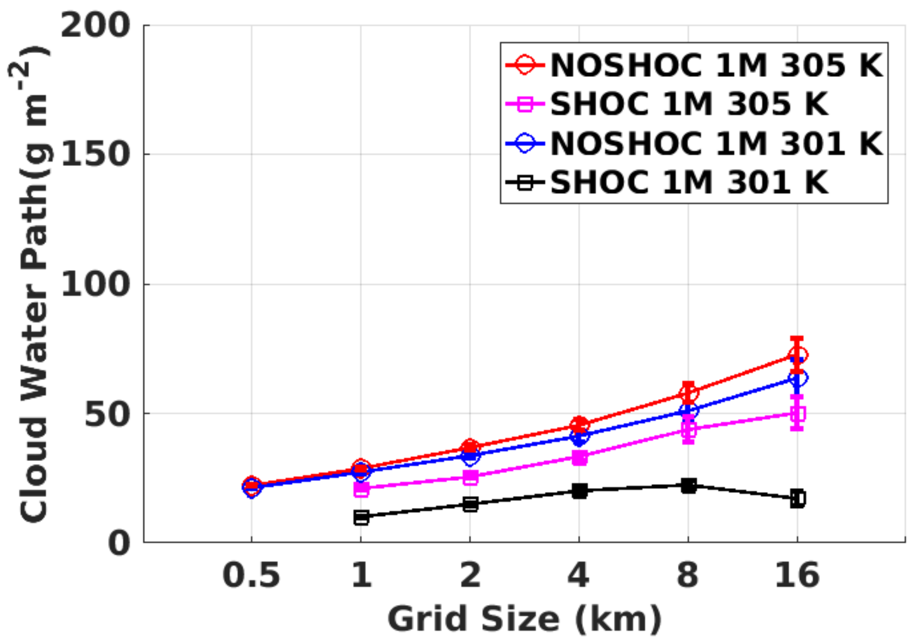

All results from final 25-day averages.

Higher CWP and much lower IWP in double-moment runs.

Single moment SHOC runs have lower CWP and IWP.

RCE Results: CWP & IWP

Single moment

Double moment

All results from final 25-day averages.

IWP

Higher CWP and much lower IWP in double-moment runs.

Single moment SHOC runs have lower CWP and IWP.

SHOC 301 K runs have very little grid spacing dependence for CWP.

CWP

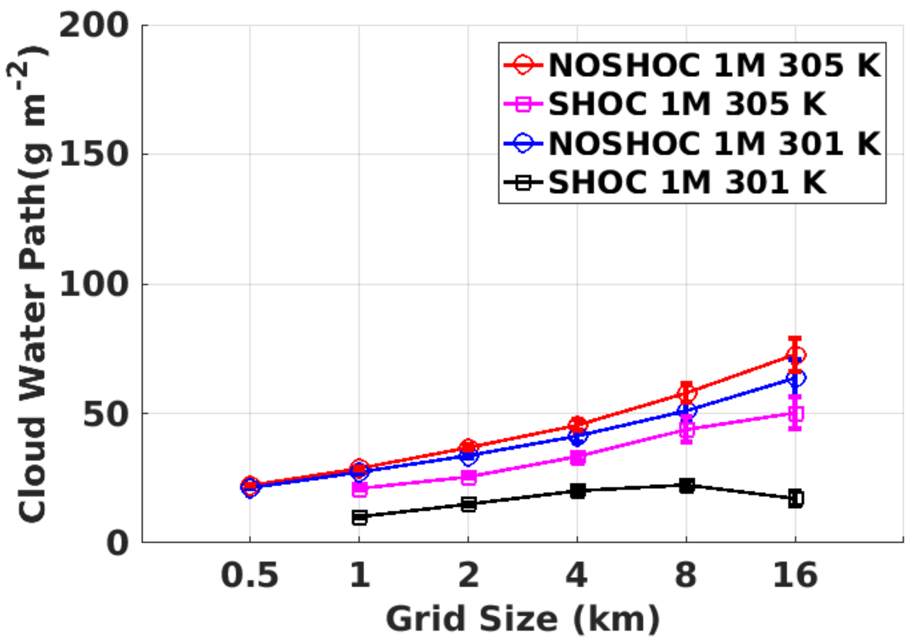

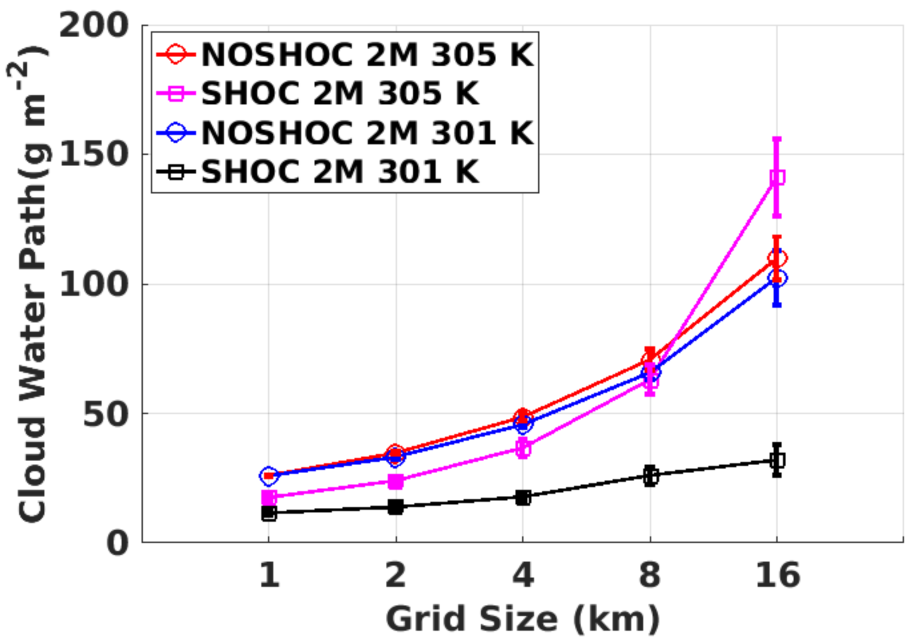

RCE Results: CWP & IWP

All results from final 25-day averages.

Single moment

Double moment

IWP

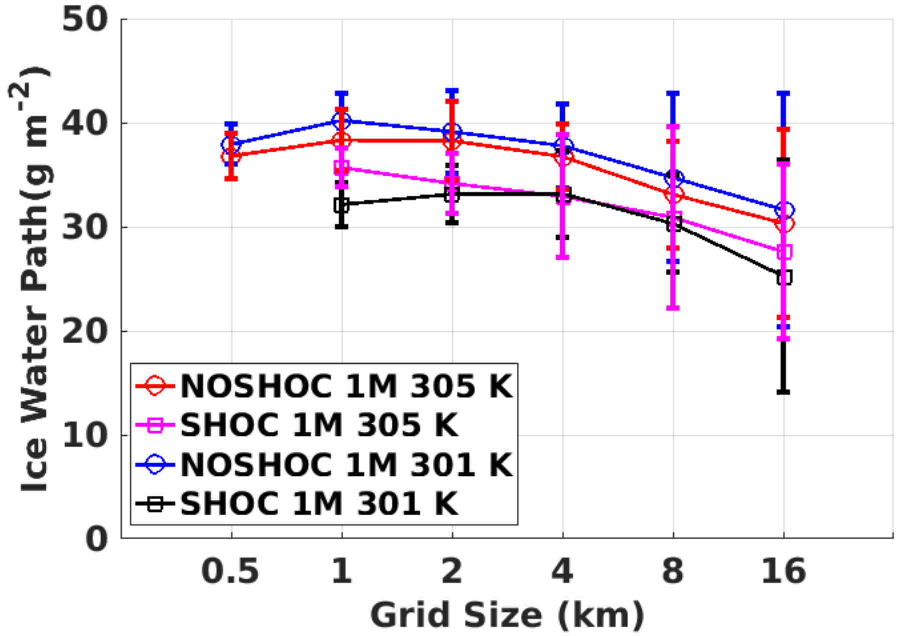

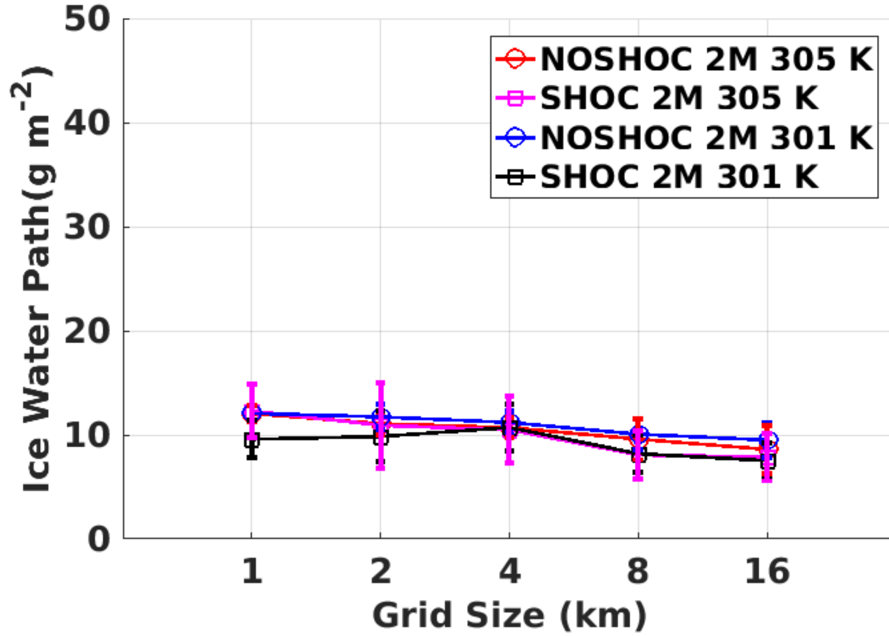

CWP

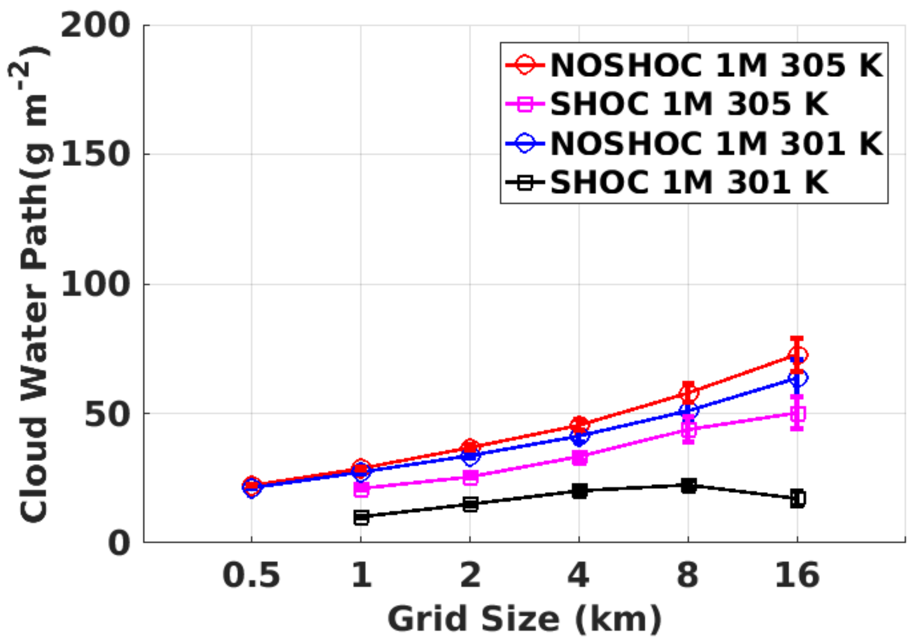

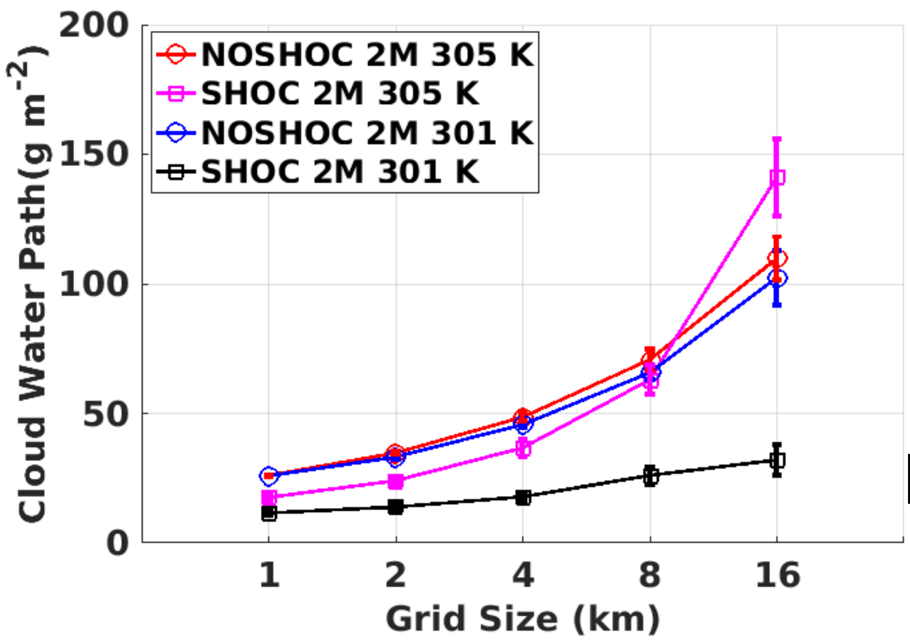

Higher CWP and much lower IWP in double-moment runs.

Single moment SHOC runs have lower CWP and IWP.

SHOC 301 K runs have very little grid spacing dependence for CWP.

Larger grid spacing -> lower IWP & higher CWP.

RCE Results

Single moment

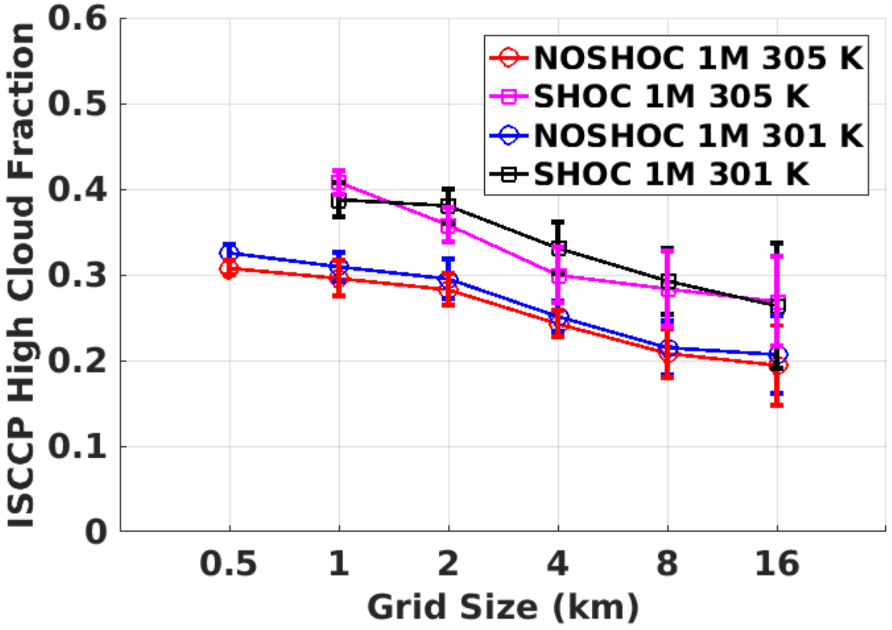

Double moment

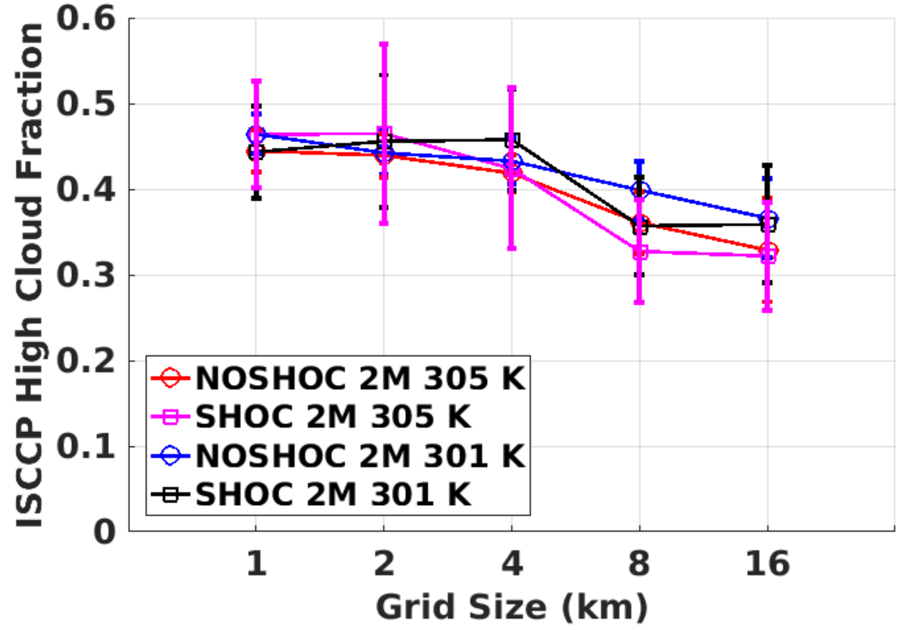

High cloud fractions higher for double moment than single moment.

High Cloud

Low Cloud

RCE Results

Single moment

Double moment

High Cloud

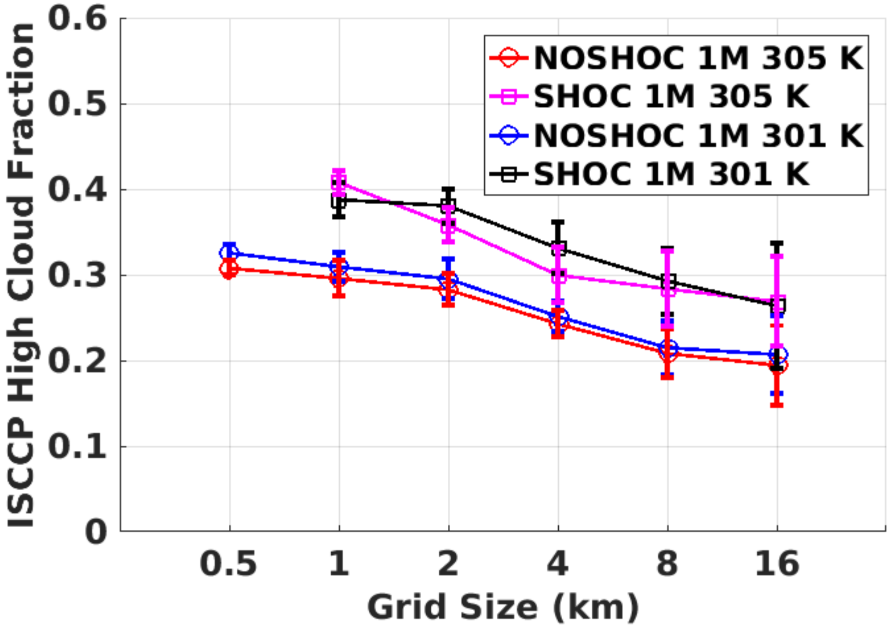

Low Cloud

High cloud fractions higher for double moment than single moment.

Single moment SHOC runs have higher high cloud fraction despite lower IWP.

RCE Results

Single moment

Double moment

High Cloud

Low Cloud

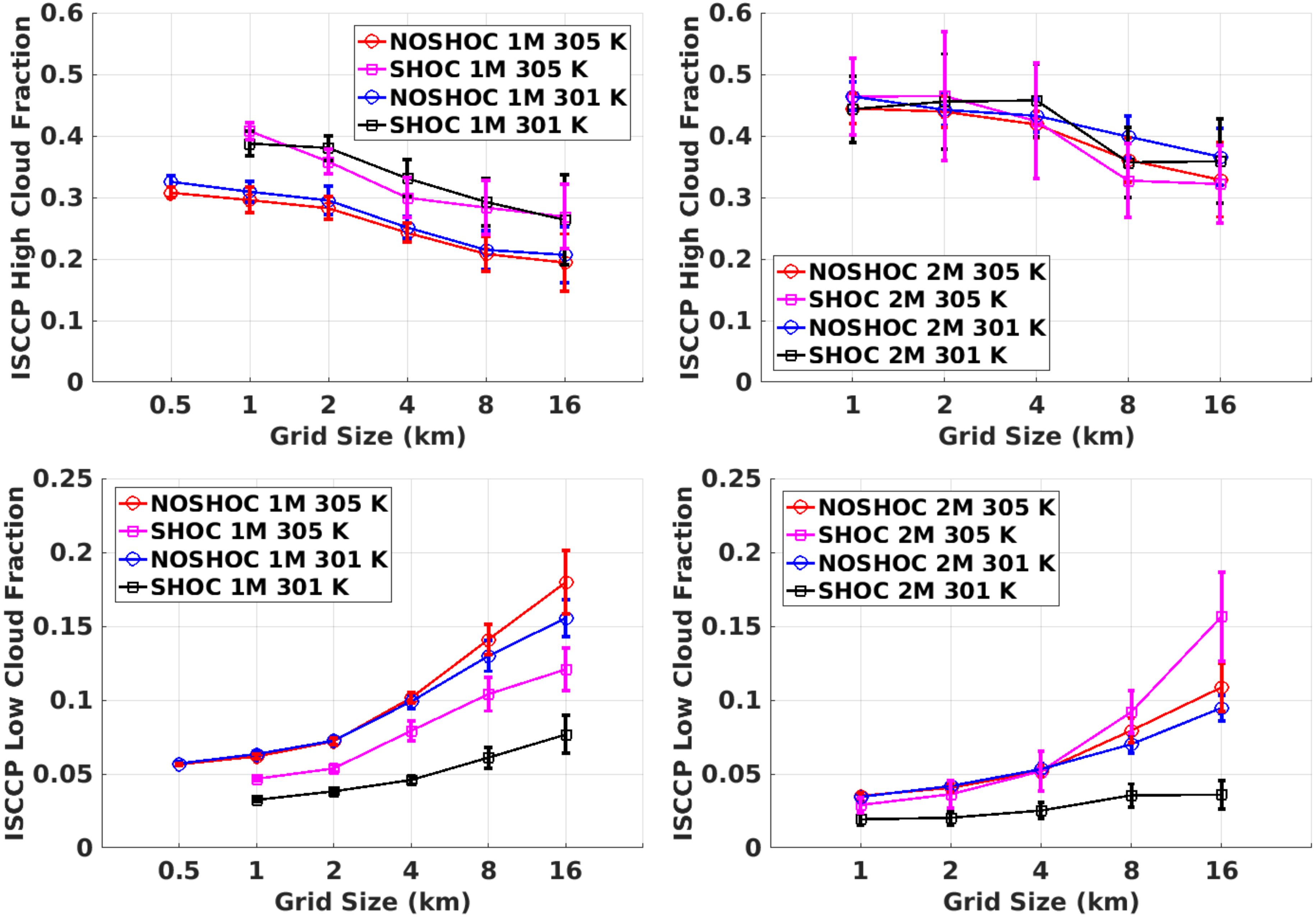

High cloud fractions higher for double moment than single moment.

Single moment SHOC runs have higher high cloud fraction despite lower IWP.

Grid size and SST dependencies similar to CWP and IWP.

RCE Results

For the cloud forcing, eight additional 1 km runs on 64 km domains were performed with ISCCP cloud histograms generated.

Cloud radiative kernels were used to generate climate feedbacks.

Kernels selected were created from ERA Interim data (Zhou et al., 2013). Zelinka et al. (2012a,b) kernels also considered.

$$LW_{feedback} = (LWCF_{(305\ K)} - LWCF_{(301K)}) / 4$$

$$SW_{feedback} = (SWCF_{(305\ K)} - SWCF_{(301K)}) / 4$$

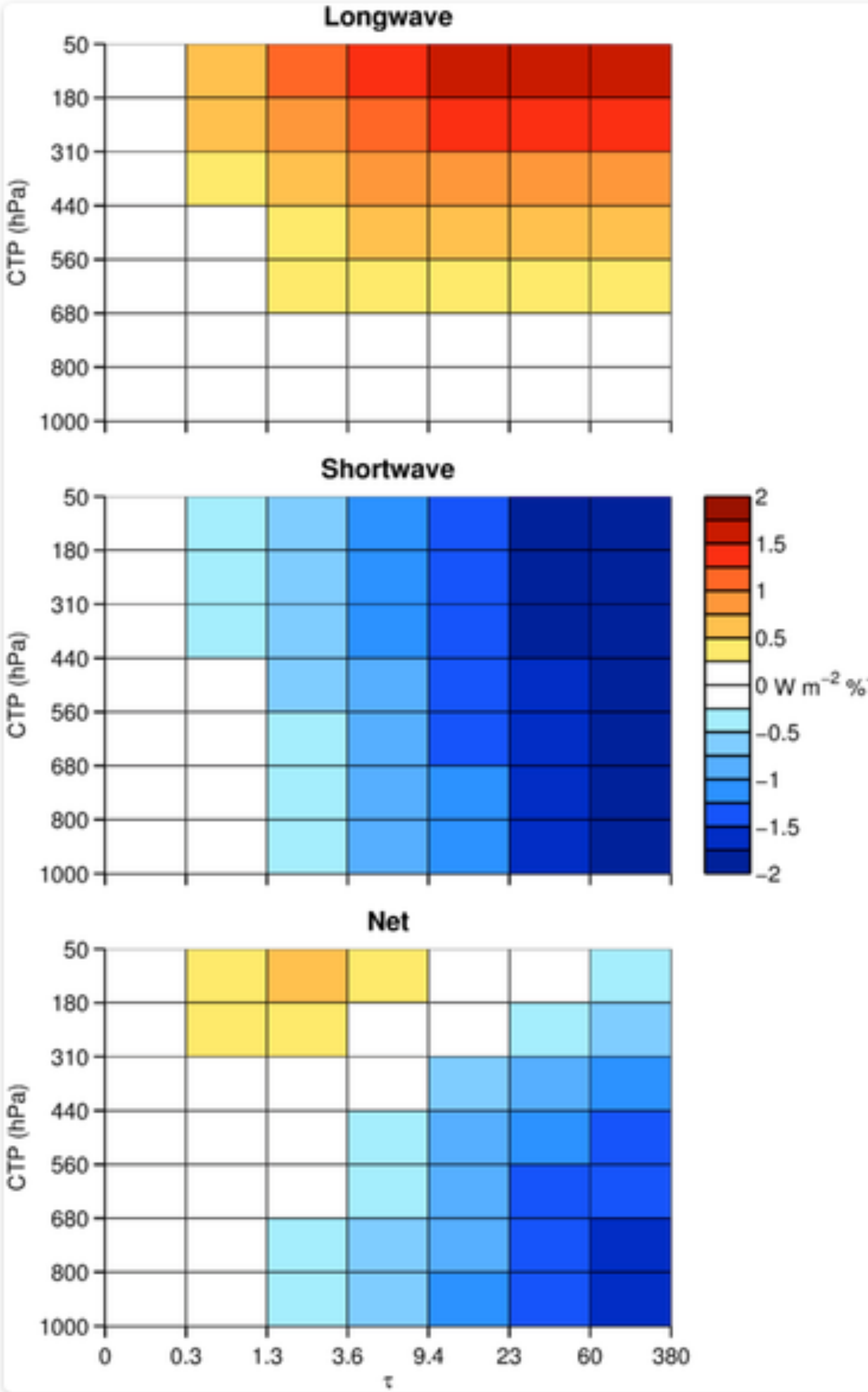

Image: Cloud radiative kernels in Figure 1 of Zelinka et al (2012a)

RCE Results: Cloud Fraction

NOSHOC

SHOC

305 K

301 K

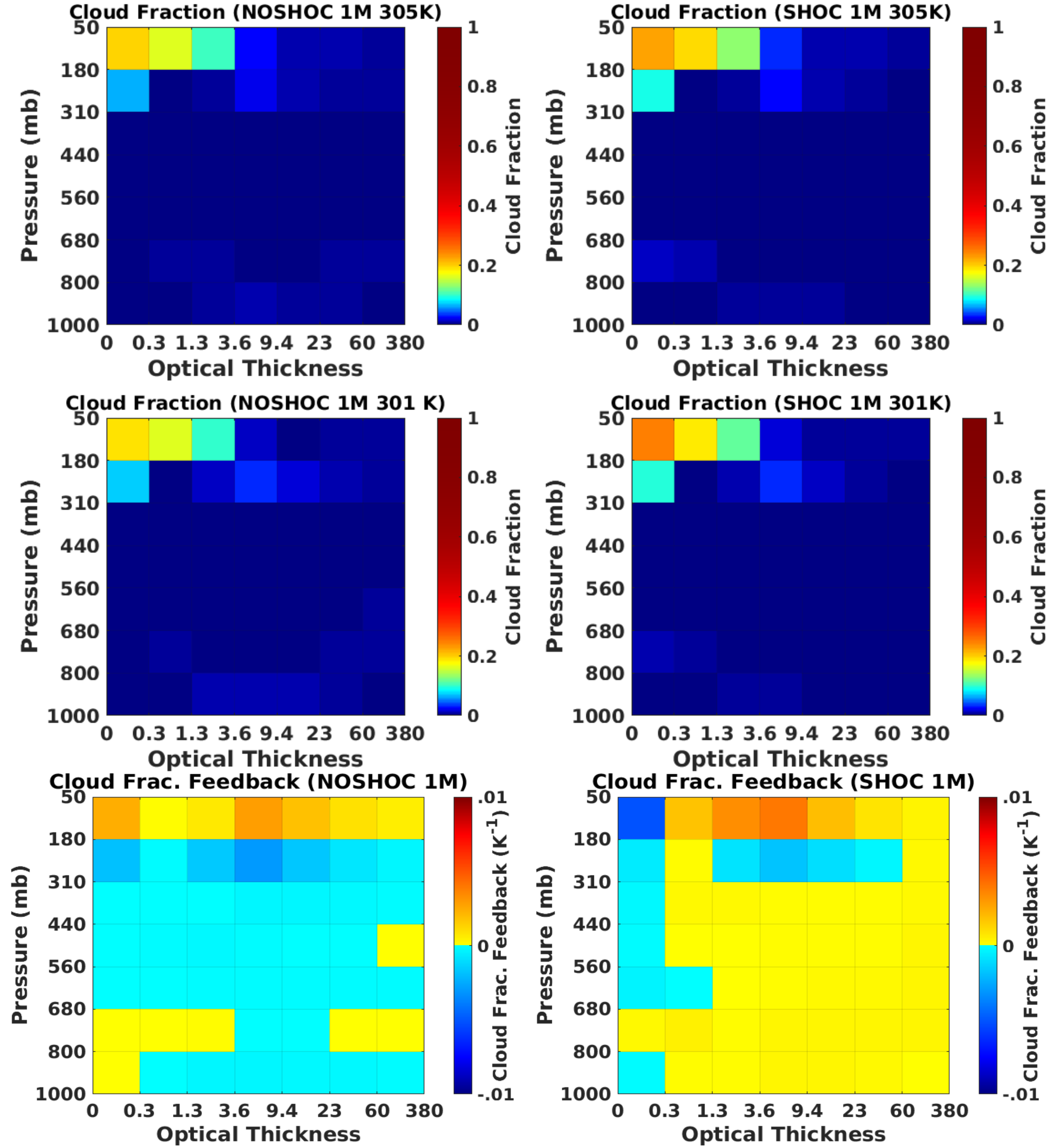

Upper level cirrus is the predominant cloud type.

Cloud fraction shifts to highest altitude bins with warming.

SHOC also has a small increase throughout low-mid levels with warming.

RCE Results: LW Cloud Forcing

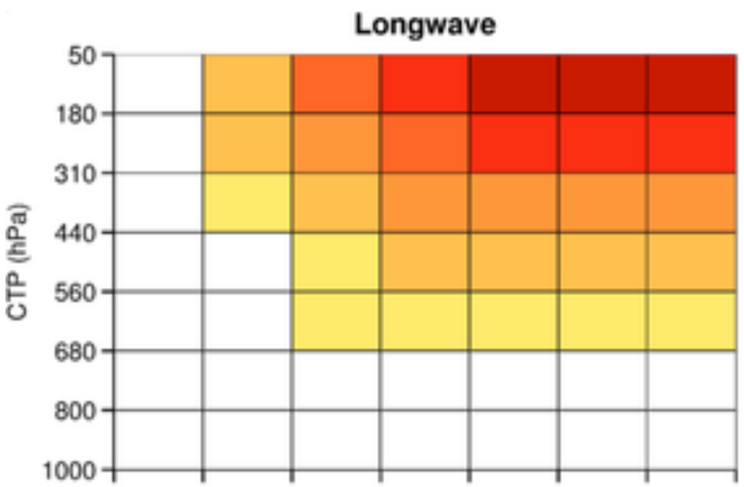

Zelinka et al (2012a)

LW forcing pattern similar to cloud fraction with a larger influence in high level/large optical thickness bins.

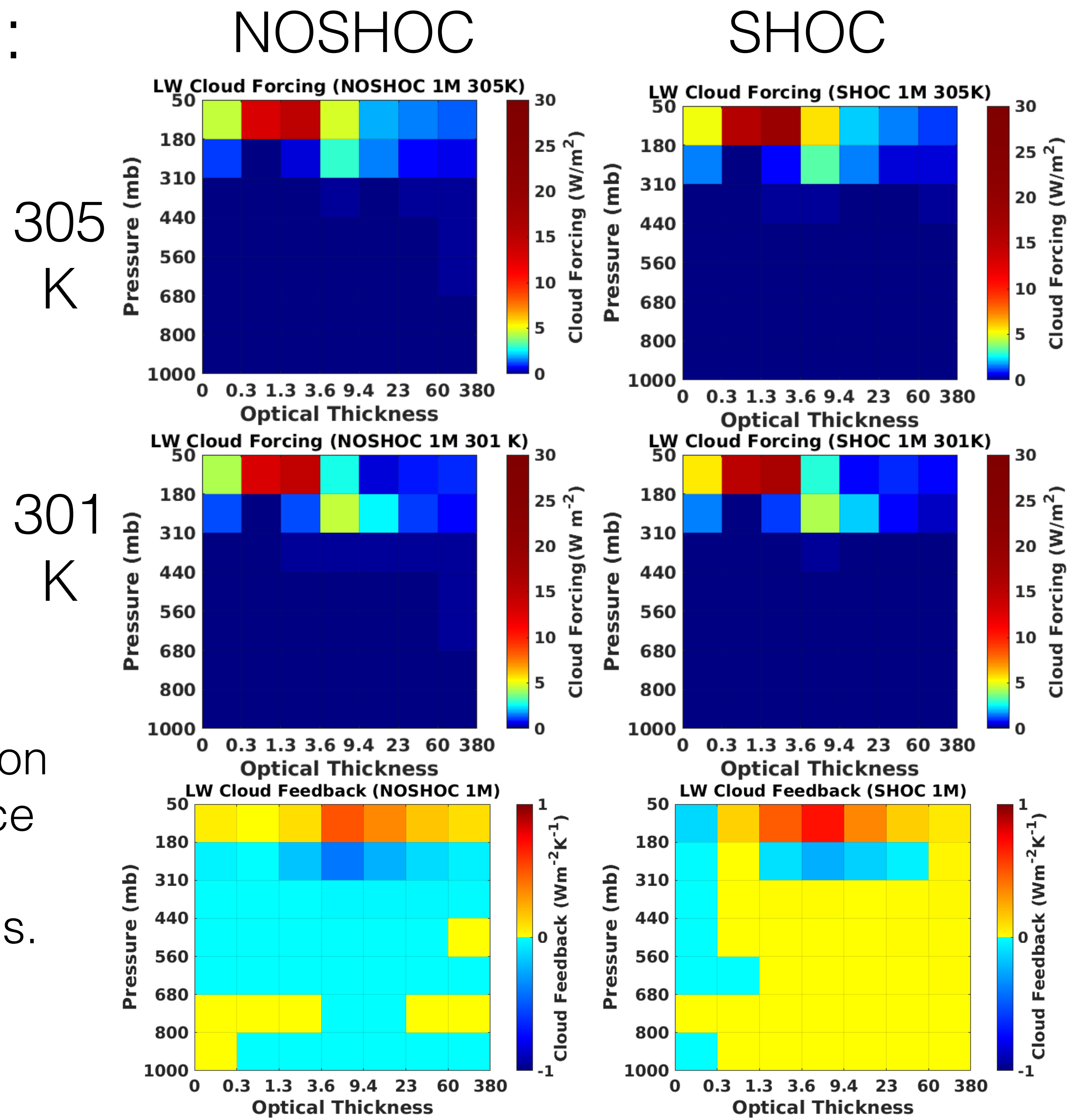

RCE Results: -1*SW Cloud Forcing

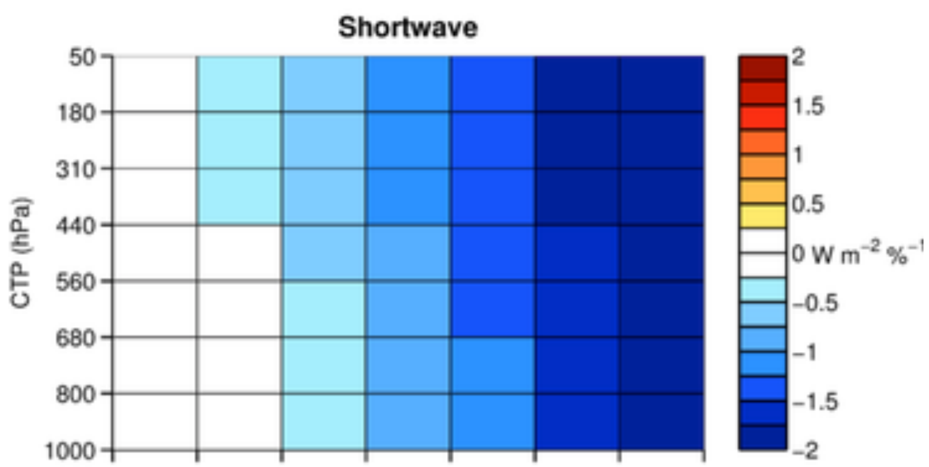

Zelinka et al (2012a)

NOSHOC

SHOC

305 K

301 K

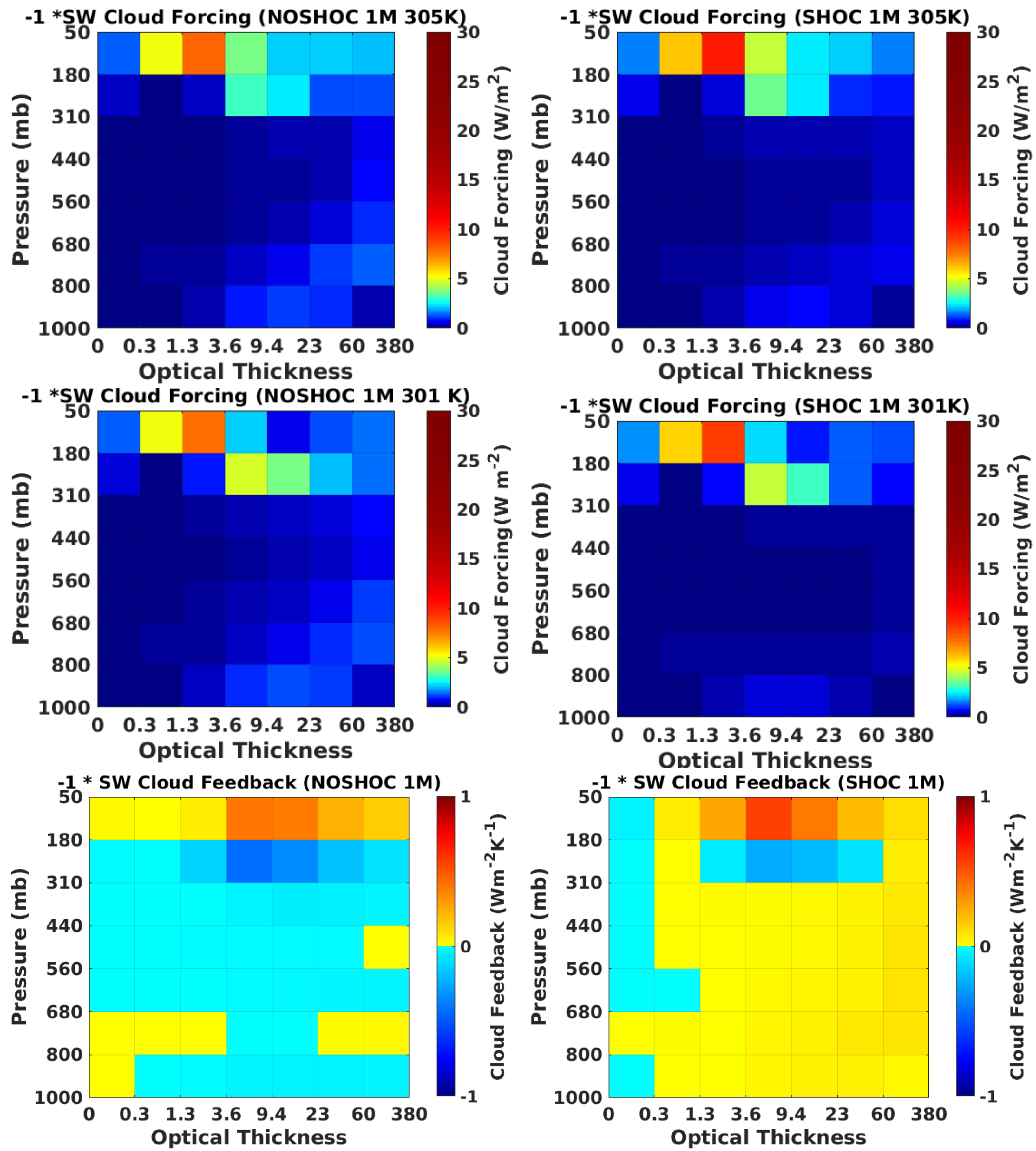

SW forcing pattern similar to cloud fraction with a larger influence in large optical thickness bins.

RCE Results: Net Cloud Forcing

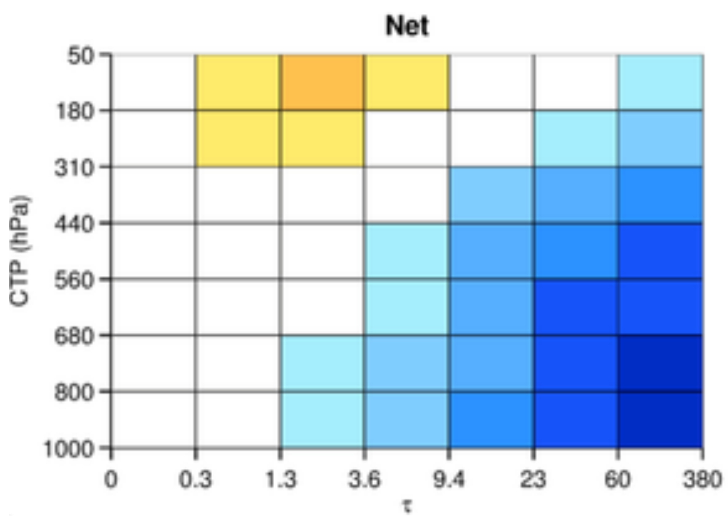

Zelinka et al (2012a)

Most positive/negative net cloud forcing is upper-level cirrus/low-level cloud.

SHOC has a negative net cloud feedback in low-mid levels. NOSHOC positive.

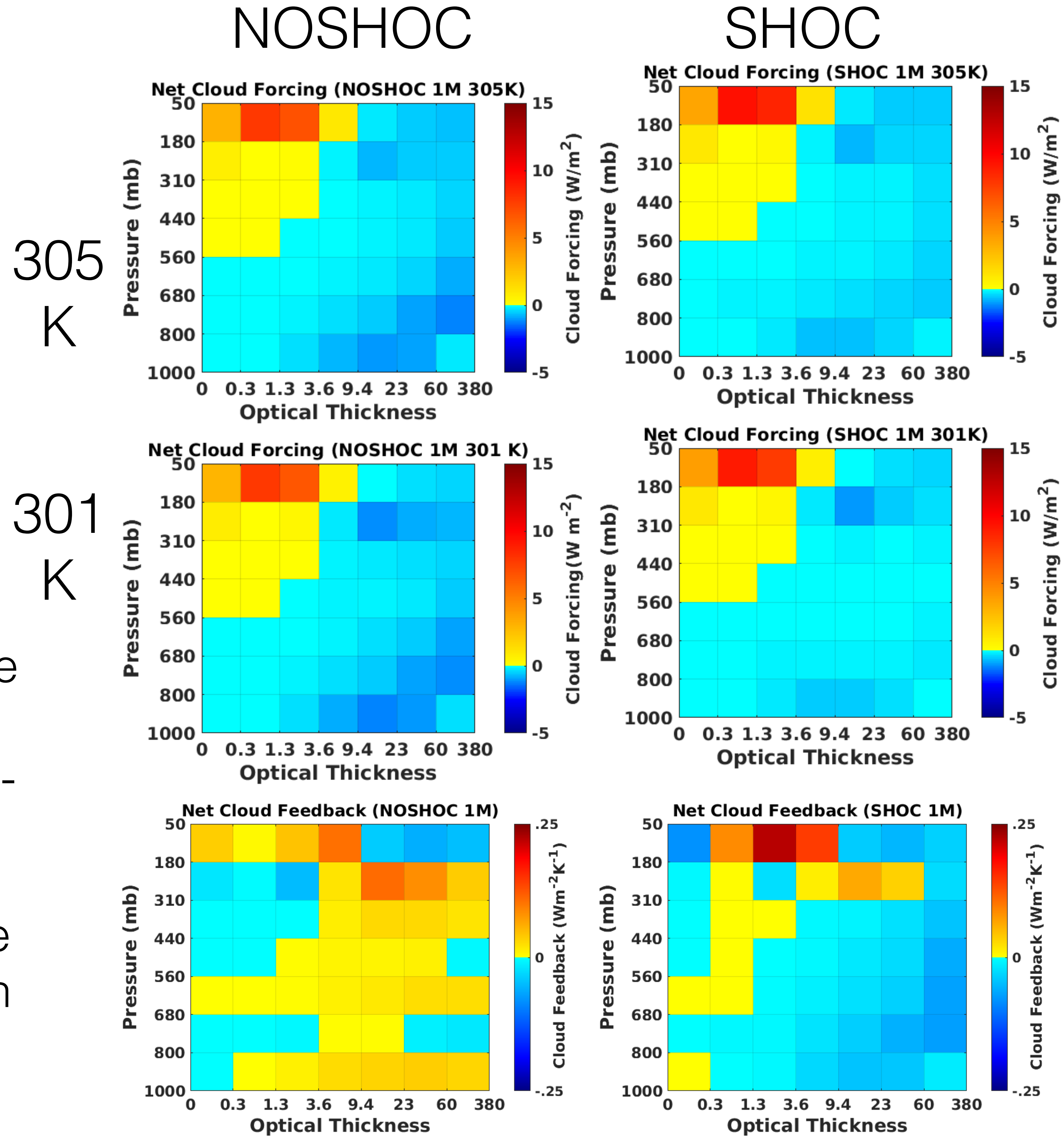

RCE Results

Cloud Feedback	1M NOSHOC	2M NOSHOC	1M SHOC	2M SHOC
LW ($W\ m^{-2}\ K^{-1}$)	0.16	-0.23	1.46	1.16
SW ($W\ m^{-2}\ K^{-1}$)	0.36	0.17	-1.82	-1.51
Net ($W\ m^{-2}\ K^{-1}$)	0.52	-0.06	-0.36	-0.35

Magnitude of cloud feedback values (LW and SW) is much higher for SHOC than NOSHOC.

Sign is opposite for 1M NOSHOC net cloud feedback compared to SHOC net cloud feedback.

RCE Summary

-Grid size has a large impact, particularly for CWP and low cloud.

-Microphysics scheme has a large impact on CWP vs IWP.

-Upper-level cirrus is primary cloud type and primary contributor to cloud forcing.

-Net cloud feedback positive for NOSHOC, negative for SHOC.

-Low-mid troposphere responsible for negative SHOC net cloud feedback.

DYNAMO - Background

Dynamics of the Madden-Julian Oscillation (DYNAMO)

Field campaigns late 2011-early 2012 in Indian Ocean and Western Pacific.

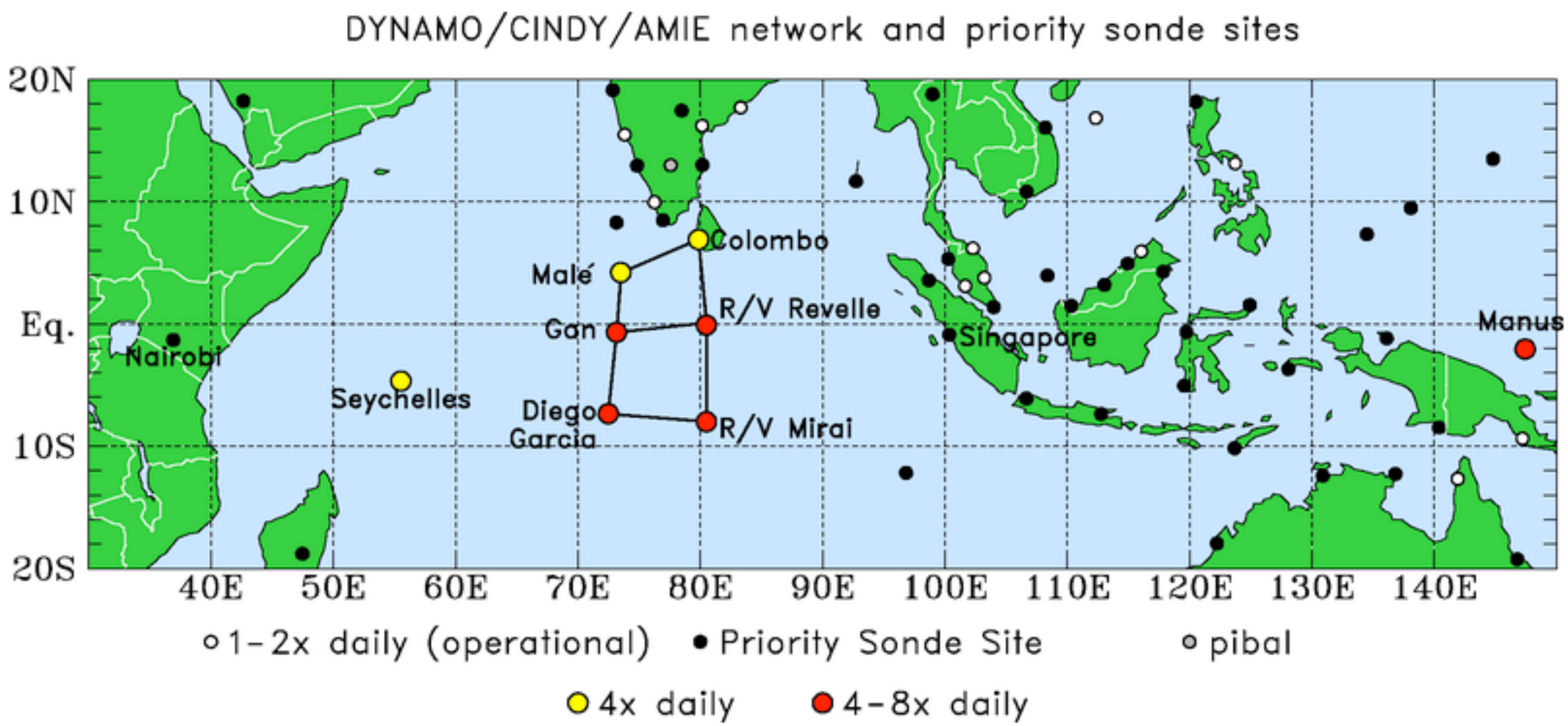

From: Johnson and Cieselski (2013)

DYNAMO - Background

-MJO cycle: suppressed phase -> cumulus congestus -> deep convection -> stratiform precipitation -> suppressed phase (Bladé and Hartmann, 1993, Benedict and Randall, 2007).

-Shallow cumulus more prominent during suppressed phase.

-General circulation models have had difficulty moistening troposphere by shallow convection (Del Genio et al., 2012).

DYNAMO - Background

-Gan Island ARM mobile facility at 0° 41′ S, 73° 9′ E.

-KAZR radar located at AMF.

-S-PolKa radar ~9km away.

DYNAMO - Case Selection

Two shallow cumulus cases were selected:

1. 00z 13 October 2011 - 12z 14 October 2011
- during cumulus congestus transition period
- other cloud types present along with shallow Cu

2. 00z 4 November 2011 - 00z 7 November 2011
- calm suppressed period of the MJO
- little presence of other cloud types

DYNAMO - Case Selection

Case 1: 00z 13 October 2011 - 12z 14 October 2011

0430z 13 October

0700z 13 October

0930z 13 October

0430z 14 October

0700z 14 October

0930z 14 October

ARM Total Sky Imager data from Gan Island (Morris, 2005; ARM Climate Research Facility, 2011a).

DYNAMO - Case Selection

Case 1: 00z 13 October 2011 - 12z 14 October 2011

-CombRet combines KAZR and S-Pol radar data (Feng et al., 2014; ARM Climate Research Facility, 2011b).
-CombRet data is at 90 m vertical resolution.
-KAZR beam width is 5.2 m at 1 km (Widener et al. 2012).
-KAZR has much higher resolution and is primary influence on CombRet.
-S-Pol influences the CombRet precipitation.

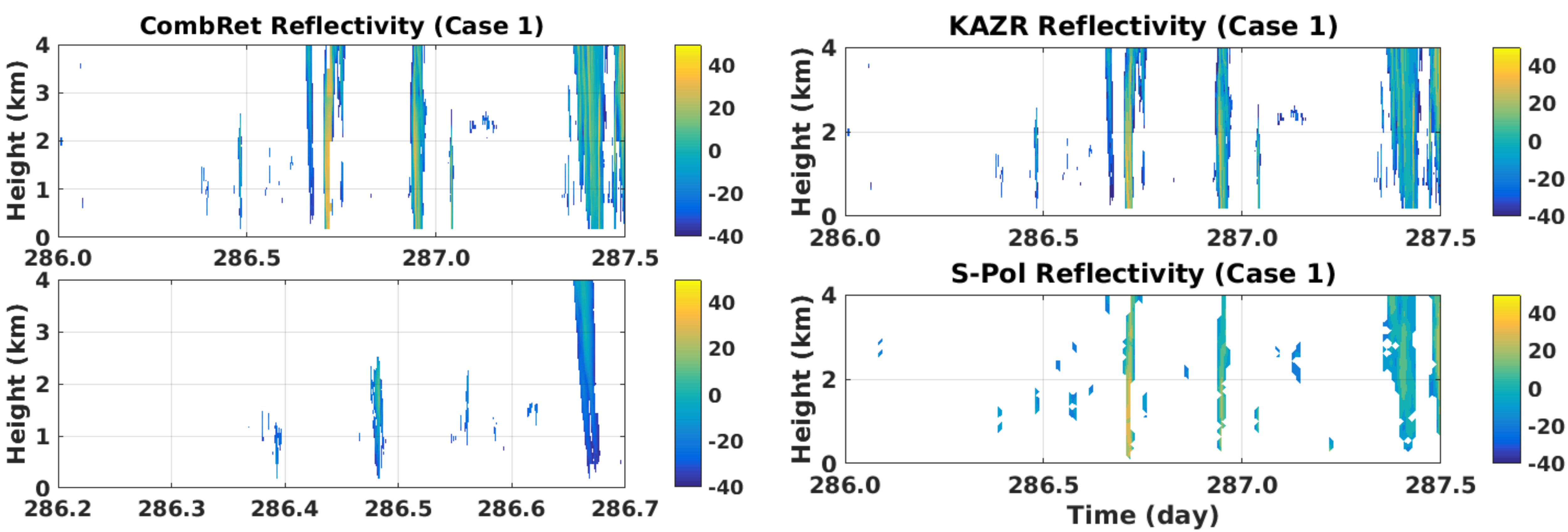

DYNAMO - Case Selection

Case 2: 00z 4 November 2011 - 00z 7 November 2011

0430z 4 November 2011

0730z 4 November 2011

0430z 5 November 2011

0730z 5 November 2011

0430z 6 November 2011

0730z 6 November 2011

DYNAMO - Case Selection

Case 2: 00z 4 November 2011 - 00z 7 November 2011

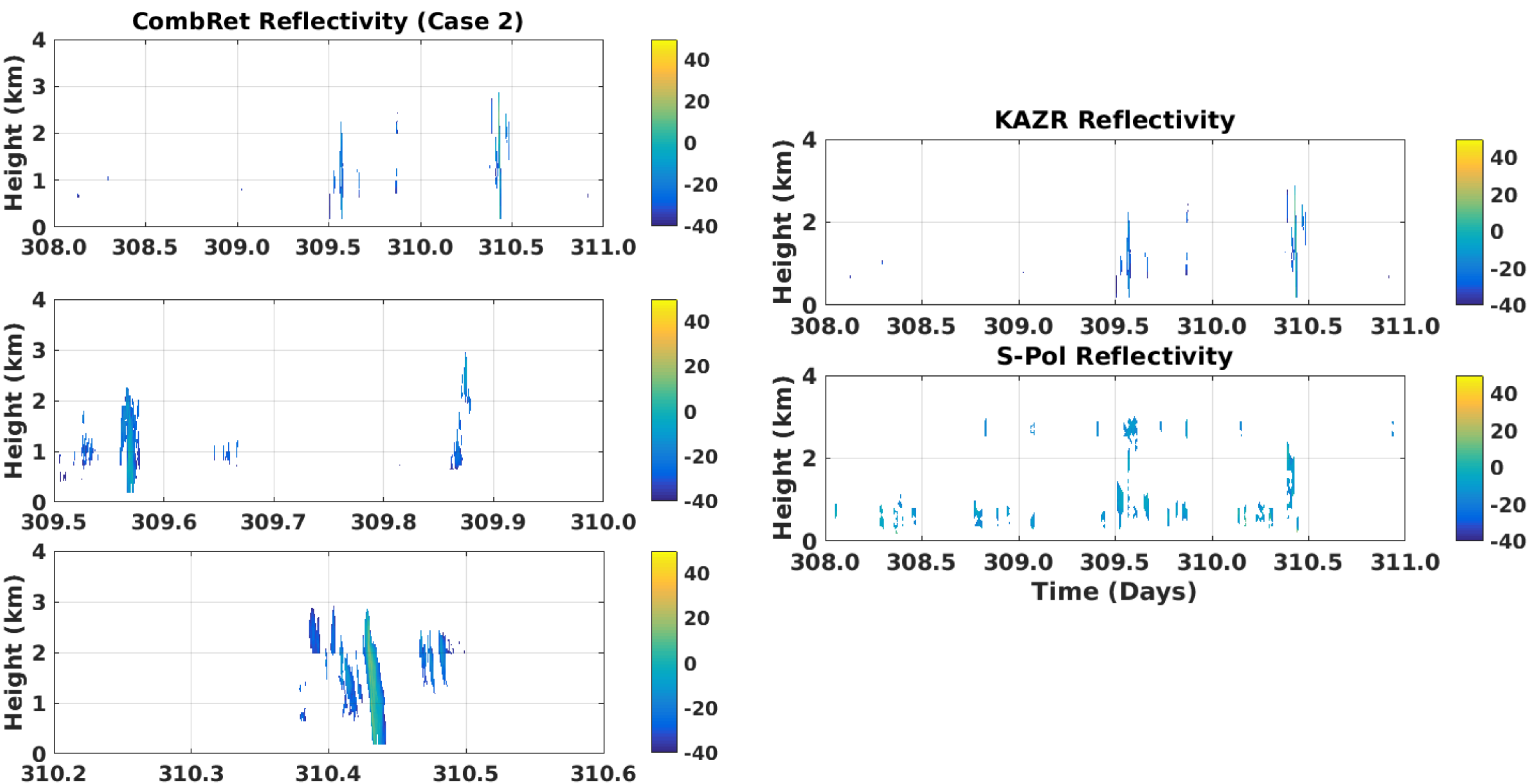

DYNAMO - Model Runs

Cloud resolving model runs used forcing derived from:

-Gan ECMWF analysis (Zhang and Lin, 1997; Zhang et al., 2001)

-TRMM precipitation radar estimates

-SSTs from the NOAA 1/4° Optimum Interpolation Sea Surface Temperature (OISST) satellite product (Reynolds et al., 2007; Reynolds, 2009)

Case	Days	H. Spacing	Domain	# V. Levels	Lowest V. Level	V. Spacing
1	286-287.5	2 km	64 km	67	50 m	100 m
1	286-287.5	1 km	32 km	67	50 m	100 m
1	286-287.5	0.5 km	32 km	109	25 m	50 m
1	286-287.5	0.1 km	32 km	109	25 m	50 m
2	304-307	2 km	64 km	67	50 m	100 m
2	304-307	1 km	32 km	67	50 m	100m
2	304-307	0.5 km	32 km	109	25 m	50 m
2	304-307	0.1 km	32 km	109	25 m	50 m

DYNAMO - Results

Case 1 500m run: CWP

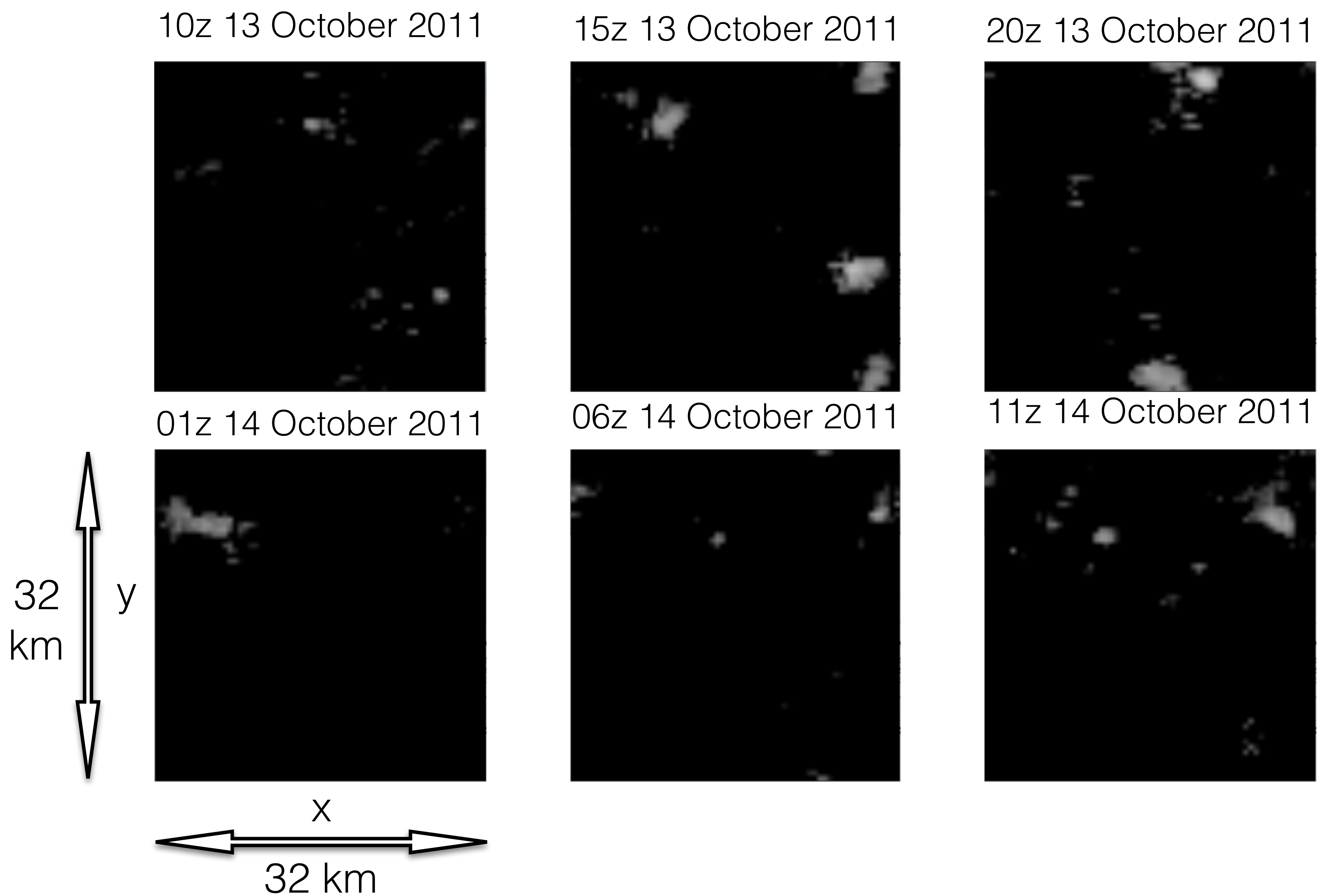

DYNAMO - Results

Case 2 500m run: CWP

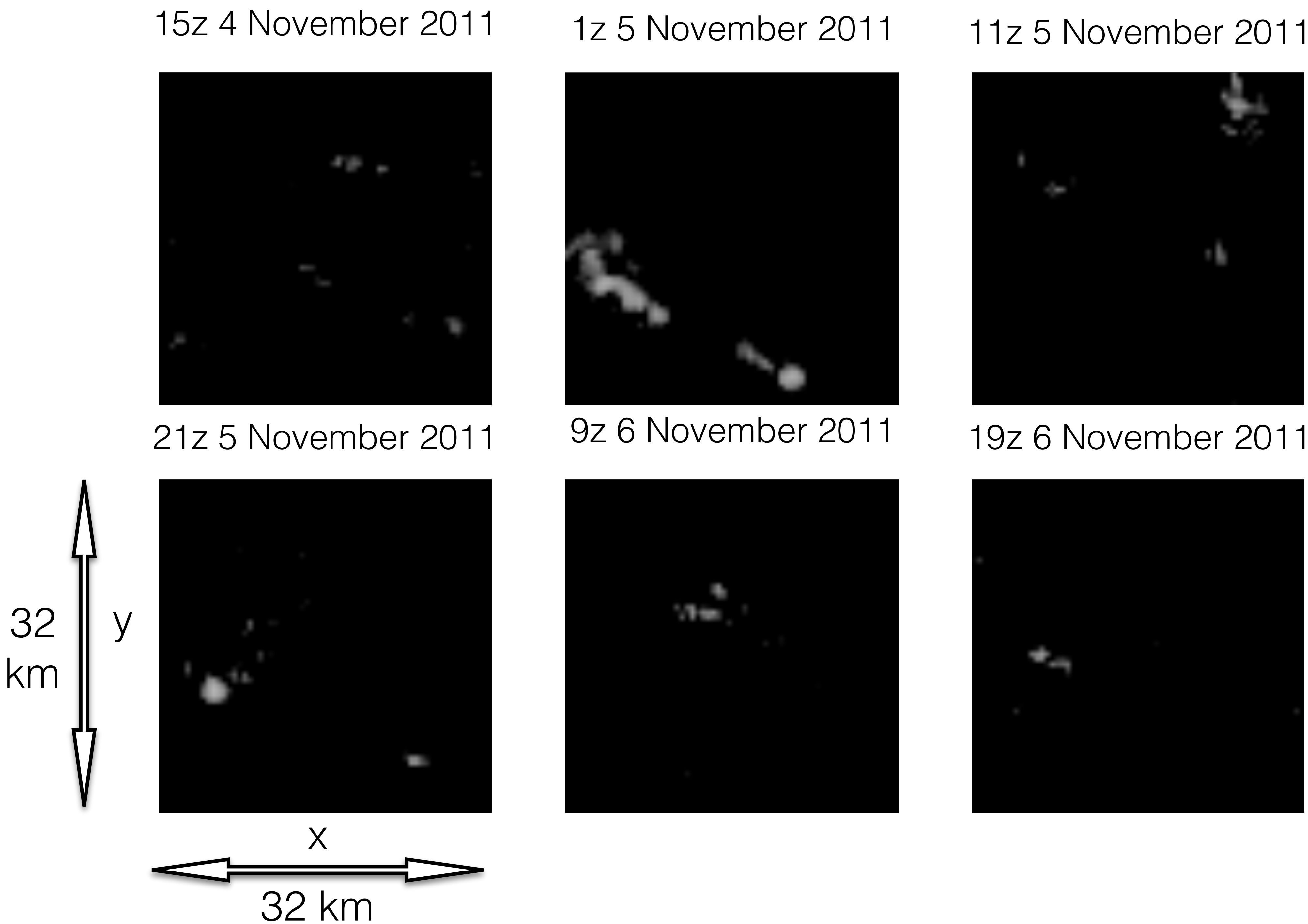

DYNAMO - Results

-Comparing to observation reflectivity values requires a model reflectivity estimate.

-Model reflectivity values were calculated using mixing ratios (cloud water, ice, snow, rain, graupel) and number concentrations.

-Method based on Morrison et al. (2009) and Martin et al. (1994), detailed further by Varble (2013) and Stanford (2016).

DYNAMO - Results

Case 1 -
2 km run

Wide range in precipitation events.

All 16 points had some shallow cloud.

Model took almost 6 hr to spin-up to initial clouds.

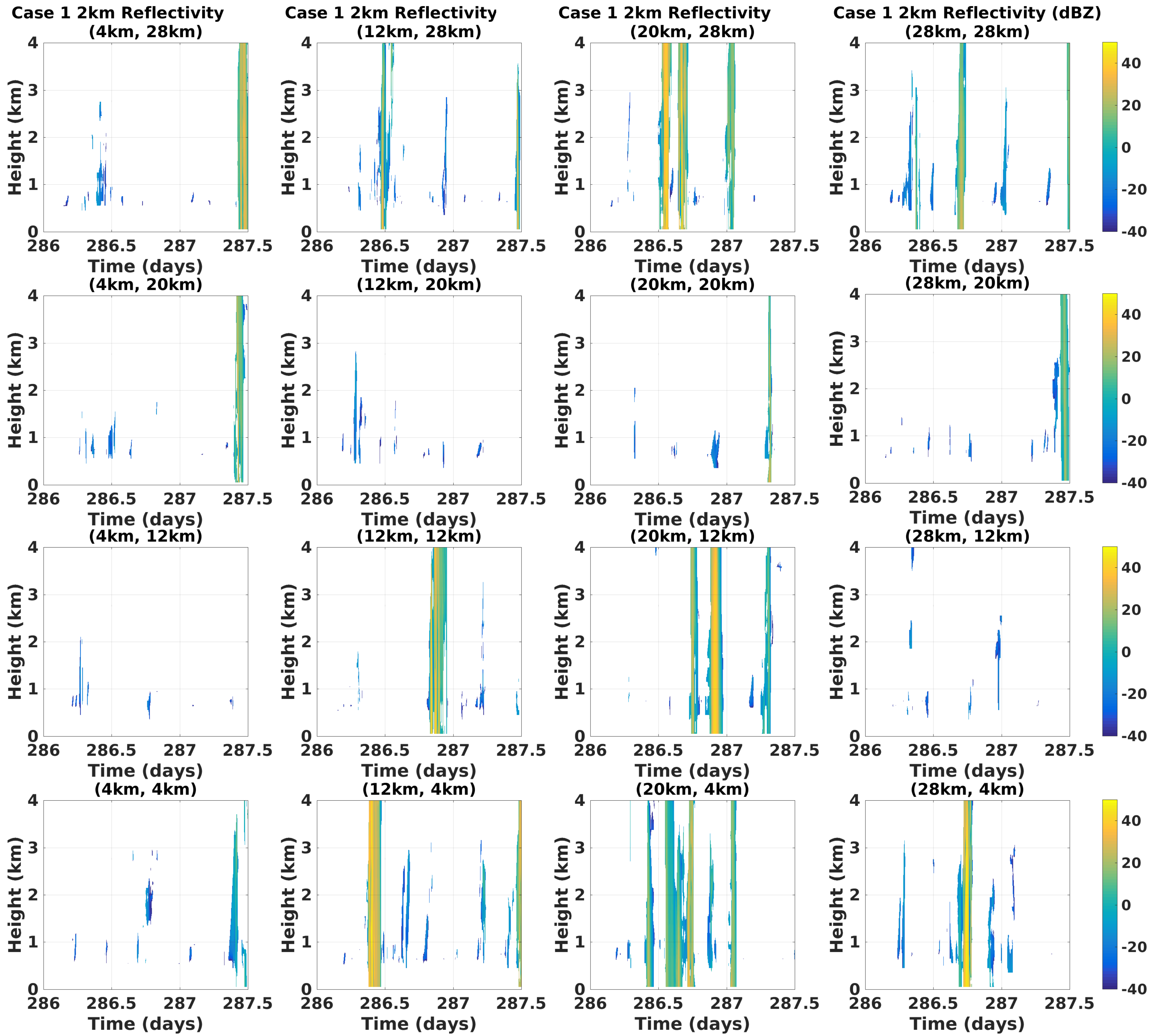

DYNAMO - Results

Case 1 -
500 m run

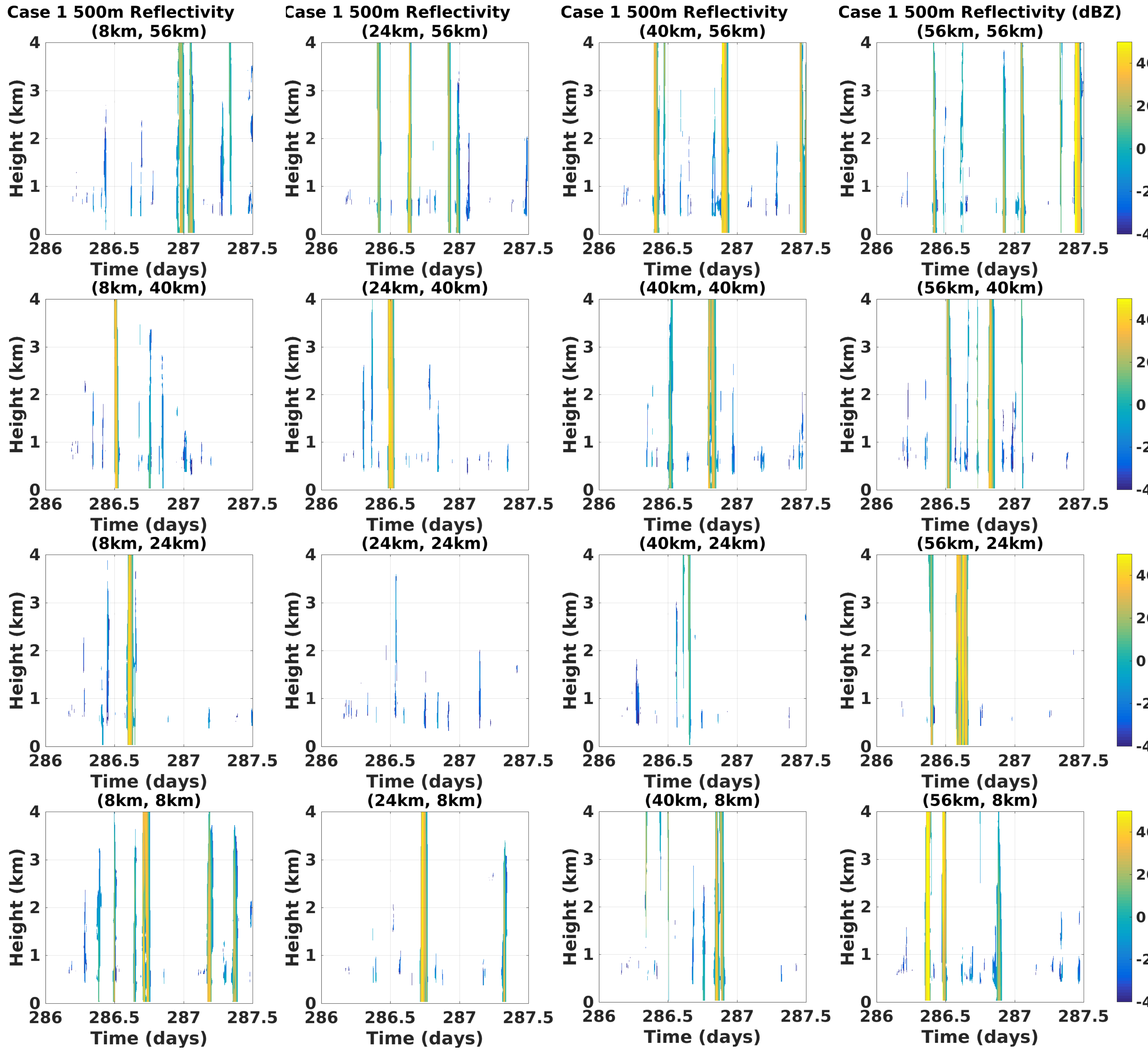

DYNAMO - Results

The percentage of time reflectivity exceeds a threshold at each grid point can be calculated.

The mean over the model can be determined.

However, to compare to a single point location, standard deviations were also calculated for the model.

DYNAMO - Results

> -40 dBZ   > -30 dBZ   > -20 dBZ

Case 1 - 2 km run

-Low-level cloud represented well in model.

-Model has a maximum at low levels while observation profile increases w/ altitude.

-2 km run better at low levels and higher up.

Case 1 - 500 m run

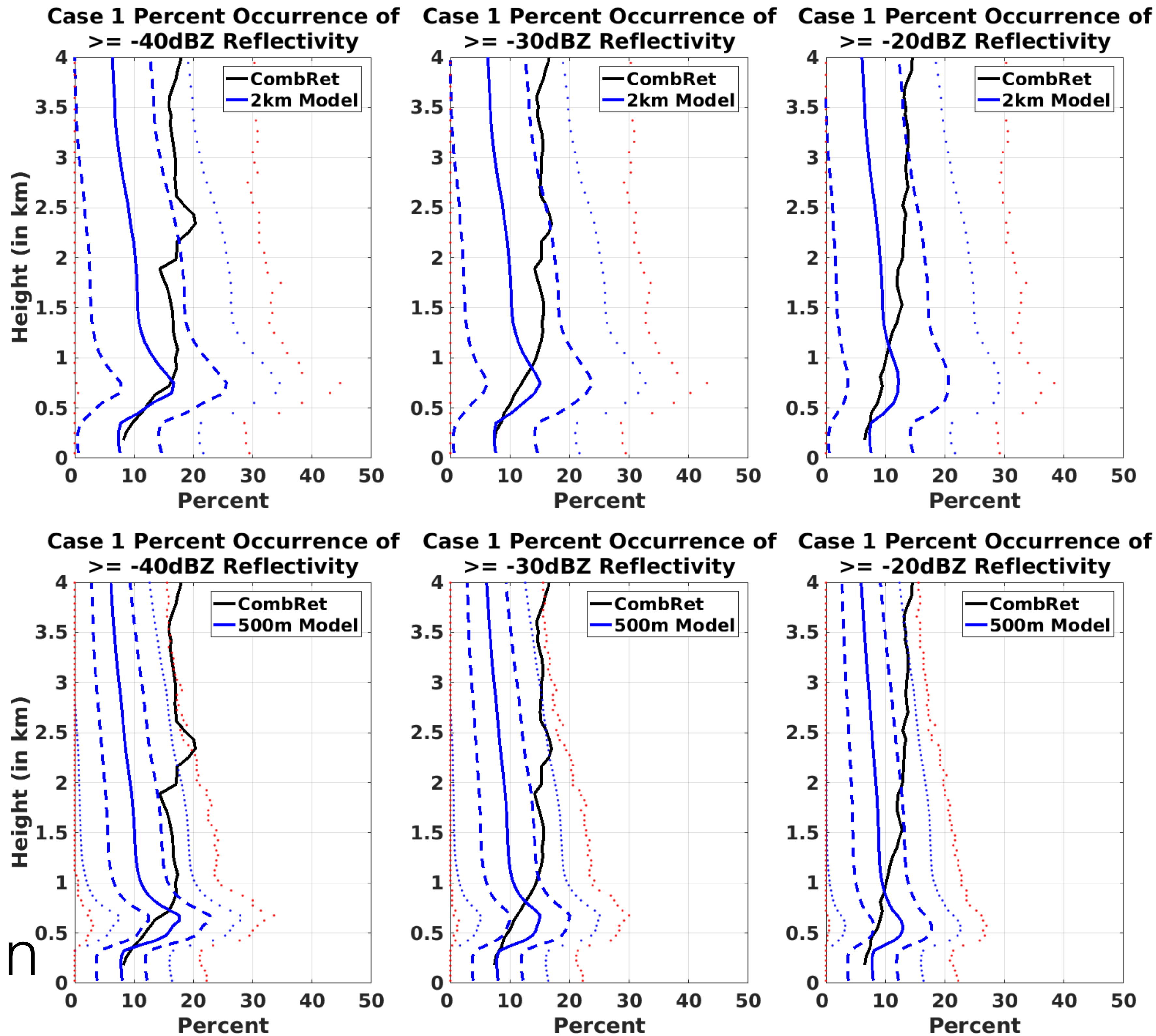

DYNAMO - Results

Case 2 -
2 km run

Much less frequent precipitation.

Model took almost 12 hours to spin up clouds.

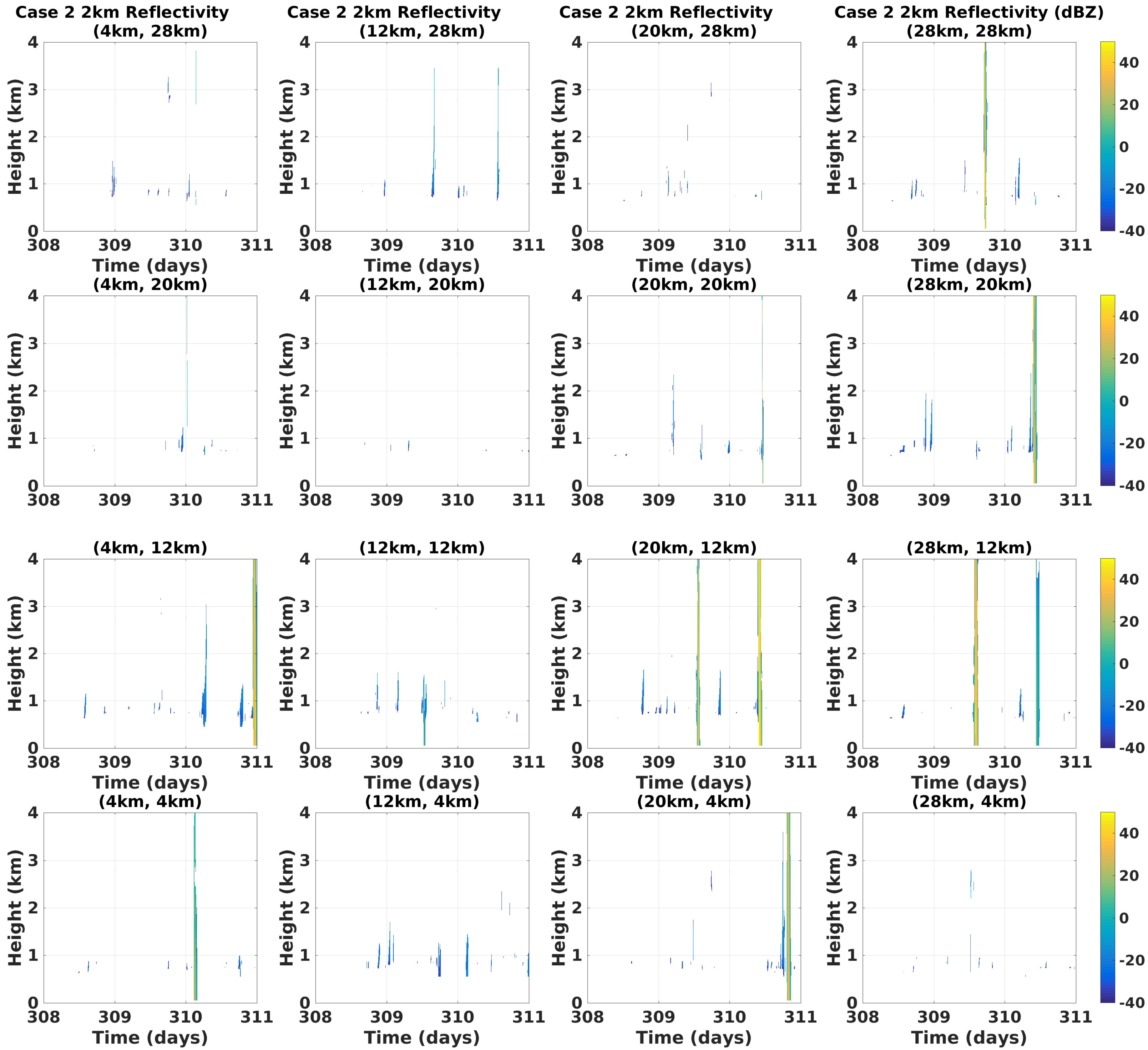

DYNAMO - Results

Case 2 -
500 m run

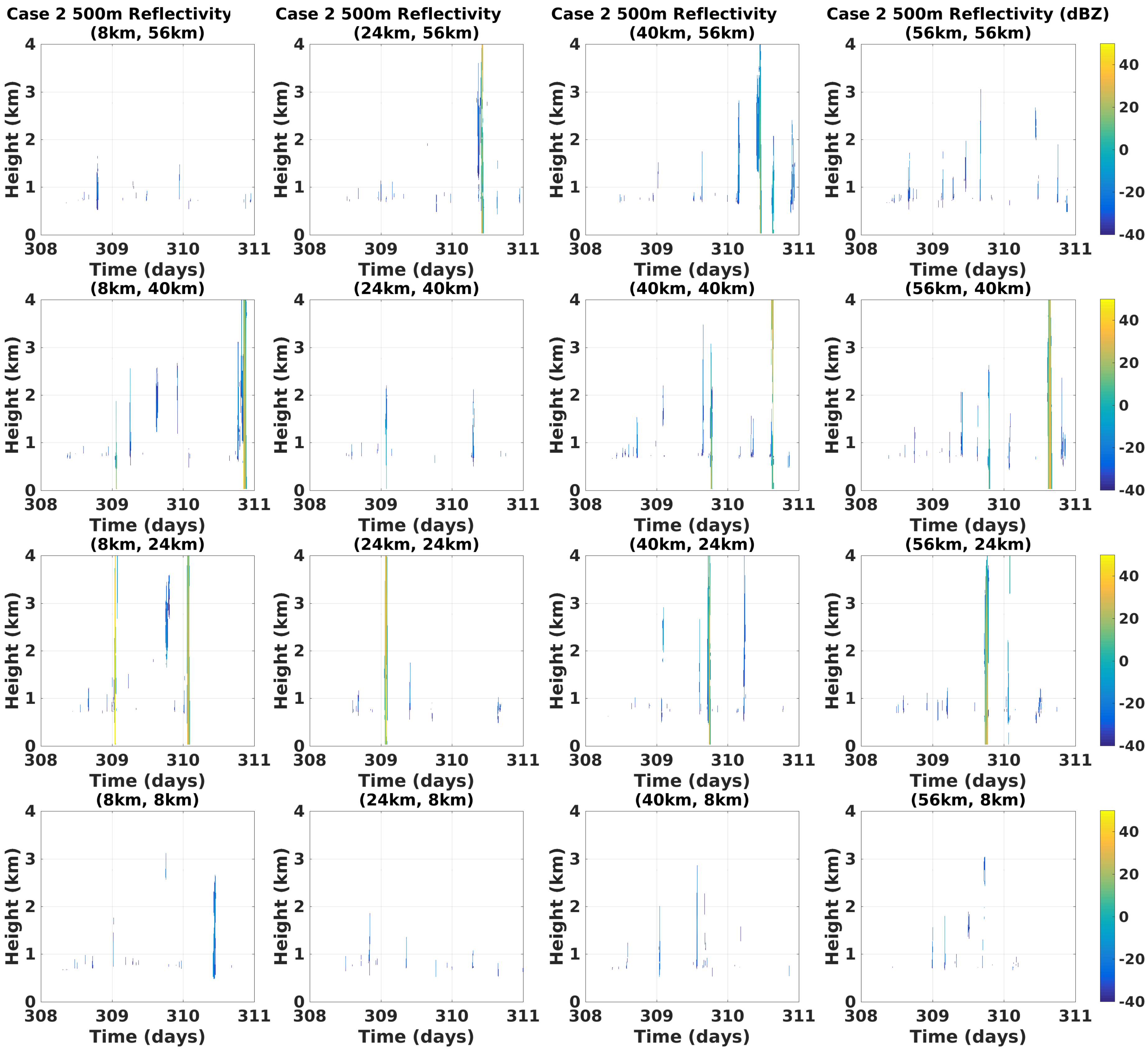

DYNAMO - Results

> -40 dBZ   > -30 dBZ   > -20 dBZ

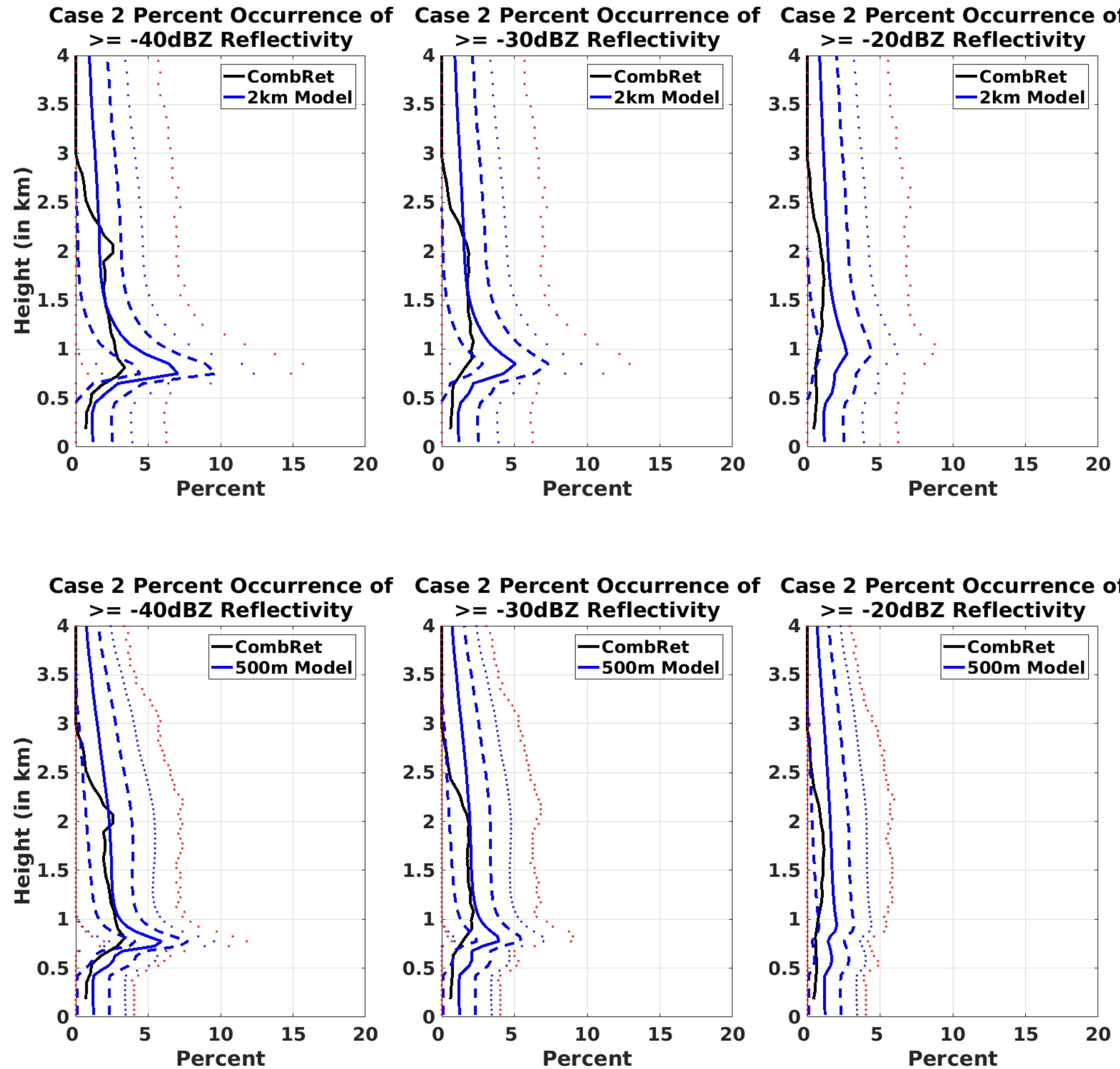

Case 2 - 2 km run

-Low-level cloud is somewhat overestimated.

-Above the observations stay within 1 stdev.

-500 m run does not overestimate low-level cloud as much and does well > -20dBZ.

Case 2 - 500 m run

DYNAMO - Results

Additional runs at 100 m grid spacing had large overestimates of shallow cumulus in both cases.

SHOC runs at 100 m showed the same result.

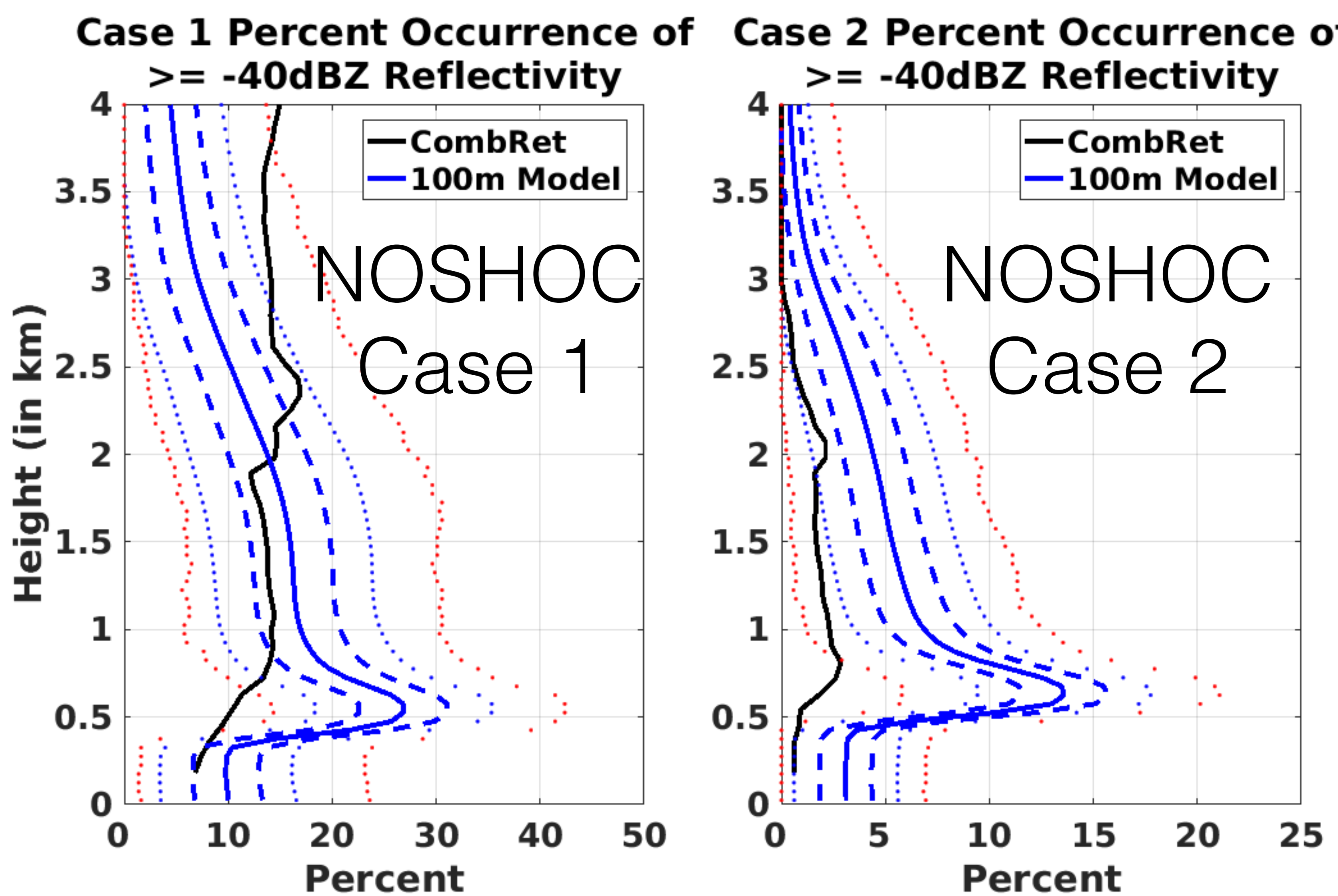

DYNAMO - Summary

-Limited frequency of shallow cumulus events with substantial coverage and few clouds of other types.

-Cloud resolving model scales represented shallow cumulus reasonably well.

Conclusions

CONSTRAIN:

-Radiation and precipitation influences on cloud cover were of opposite sign and mostly cancel.
-A more complex microphysics scheme produced supercooled water rather than ice for a marine cold air outbreak.

RCE:

-High-cloud fraction increased and low-cloud fraction decreased for a decreasing grid spacing.
-Double-moment microphysics produces more CWP and much less IWP.
-For a warming climate NOSHOC 1M runs have a positive net cloud radiative feedback; SHOC runs have a negative net cloud radiative feedback.

DYNAMO:

-Shallow Cu events without other cloud types or precipitation are uncommon outside the suppressed MJO phase.
-Shallow Cu can reasonably be modeled on cloud resolving model scales.

Overall:

-Model runs are sensitive to a wide variety of model configurations.
-Both model physics (turbulence parameterization, microphysics) and physical (domain size, grid spacing) factors are important to take into consideration.

References

ARM Climate Research Facility, 2011a: PNNL Combined Remote Sensor (gan2combret7fengM1) 2011- 10-12 to 2011-10-15 and 2011-11-3 to 2011-11-7. ARM Mobile Facility (GAN) Gan Airport, Gan Island, Maldives, Atmospheric Radiation Measurement (ARM) Climate Research Facility Data Archive: Oak Ridge, Tennessee, USA. Data set accessed 2017-04-26.

ARM Climate Research Facility, 2011b: Total Sky Imager (TSISKYIMAGE) 2011-10-9 to 2011-12-7. ARM Mobile Facility (GAN) Gan Airport, Gan Island, Maldives; AMF2 (M1), Compiled by: V. Morris. Atmospheric Radiation Measurement (ARM) Climate Research Facility Data Archive: Oak Ridge, Tennessee, USA. Data set accessed 2017-01-26., doi: 10.5439/1025309.

Benedict, J. J. and D. A. Randall, 2007: Observed characteristics of the MJO relative to maximum rainfall. *J. Atmos. Sci.*, **64**, 2332–2354, doi:10.1175/JAS3968.1.

Bladé, I. and D. L. Hartmann, 1993: Tropical intraseasonal oscillations in a simple nonlinear model. *J. Atmos. Sci.*, **50**, 2922–2939, doi: 10.1175/1520-0469(1993)050<2922:TIOIAS>2.0.CO;2.

Bogenschutz, P. A. and S. K. Krueger, 2013: A simplified PDF parameterization of subgrid-scale clouds and turbulence for cloud-resolving models. *J. Adv. Model. Earth Syst.*, **5**, 195–211., doi:10.1002/jame.20018.

Bogenschutz, P. A., S. K. Krueger, and M. Khairoutdinov, 2010: Assumed probability density functions for shallow and deep convection. *J. Adv. Model. Earth Syst.*, **2**, 24 pp., doi: 10.3894/JAMES.2010.2.10.

Bretherton, C. S., P. N. Blossey, and M. Khairoutdinov, 2005: An energy-balance analysis of deep convective self-aggregation above uniform SST. *J. Atmos. Sci.*, **62**, 4273–4292., doi:10.1175/JAS3614.1.

Brümmer, B., 1996: Boundary-layer modification in wintertime cold-air outbreaks from the Arctic sea ice. *Bound.-Layer Meteor.*, **80**, 109–125, doi:10.1007/BF00119014.

Brümmer, B., 1999: Roll and cell convection in wintertime Arctic cold-air outbreaks. *J. Atmos. Sci.*, **56**, 2613–2636, doi:10.1175/1520-0469(1999)056<2613:RACCIW>2.0.CO;2.

Canuto, V. M., Y. Cheng, and A. Howard, 2001: New third-order moments for the convective boundary layer. *J. Atmos. Sci.*, **58**, 1169–1172., doi: 10.1175/1520-0469(2001)058<1169:NTOMFT>2.0.CO;2.

Cess, R. D., et al., 1996: Cloud feedback in atmospheric general circulation models: An update. *J. Geophys. Res.*, **101**, 12 791–12 794., doi:10.1029/96JD00822.

Cheng, A., K.-M. Xu, and B. Stevens, 2010: Effects of resolution on the simulation of boundary-layer clouds and the partition of kinetic energy to subgrid scales. *J. Adv. Model. Earth Syst.*, **2**, 21 pp., doi: 10.3894/JAMES.2010.2.3.

Collins, W. D., et al., 2004: Description of the NCAR Community Atmospheric Model (CAM 3.0). Tech. rep., NCAR Tech. Note, Note NCAR/TN-464+STR, 226 pp. doi:10.5065/D63N21CH.

Del Genio, A. D., Y. Chen, D. Kim, and M.-S. Yao, 2012: The MJO transition from shallow to deep convection in CloudSat/CALIPSO data and GISS GCM simulations. *J. Climate*, **25**, 3755–3770, doi: 10.1175/JCLI-D-11-00384.1.

Feng, Z., S. McFarlane, C. Schumacher, S. Ellis, J. Comstock, and N. Bharadwaj, 2014: Constructing a merged cloud-precipitation radar dataset for tropical convective clouds during the DYNAMO/AMIE experiment at Addu Atoll. *J. Atmos. Oceanic Technol.*, **31**, 1021–1042, doi:10.1175/JTECH-D-13-00132.1.

References

Field, P. R., R. J. Cotton, K. McBeath, A. P. Lock, S. Webster, and R. P. Allan, 2014: Improving a convection- permitting model simulation of a cold air outbreak. *J. Atmos. Sci.*, **140**, 124–138., doi:10.1002/qj.2116.

Fletcher, J., S. Mason, and C. Jakob, 2016a: The climatology, meteorology, and boundary layer structure of marine cold air outbreaks in both hemispheres. *J. Climate*, **29**, 1999–2014., doi: 10.1175/JCLI-D-15-0268.1.

Fletcher, J., S. Mason, and C. Jakob, 2016b: A climatology of clouds in marine cold air outbreaks in both hemispheres. *J. Climate*, **29**, 6677–6692., doi:10.1175/JCLI-D-15-0783.1.

Golaz, J. C., V. E. Larson, and W. R. Cotton, 2002a: A PDF-based model for boundary layer clouds. Part I: Method and model description. *J. Atmos. Sci.*, **59**, 3540–3551., doi:10.1175/1520-0469(2002)059<3540:APBMFB>2.0.CO;2.

Golaz, J. C., V. E. Larson, and W. R. Cotton, 2002b: A PDF-based model for boundary layer clouds. Part II: Model results. *J. Atmos. Sci.*, **59**, 3552–3571., doi: 10.1175/1520-0469(2002)059<3552:APBMFB>2.0.CO;2.

Hartmann, D. L., L. A. Moy, and Q. Fu, 2001: Tropical convection and the energy balance at the top of the atmosphere. *J. Climate*, **14**, 4495–4511., doi: 10.1175/1520-0442(2001)014<4495:TCATEB>2.0.CO;2.

Hobbs, P. V. and A. L. Rangno, 1998: Microstructures of low and middle-level clouds over the Beaufort Sea. *Q. J. R. Meteorol. Soc.*, **124**, 2035–2071., doi:10.1002/qj.49712455012.

Johnson, R. H. and P. E. Ciesielski, 2013: Structure and properties of Madden-Julian oscillations deduced from DYNAMO sounding arrays. *J. Atmos. Sci.*, **70**, 3157–3179., doi:10.1175/JAS-D-13-065.1.

Khairoutdinov, M. and Y. L. Kogan, 1999: A large-eddy simulation model with explicit microphysics: Validation against aircraft observations of a stratocumulus-topped boundary layer. *J. Atmos. Sci.*, **56**, 2115–2131., doi:10.1175/1520-0469(1999)056<2115:ALESMW>2.0.CO;2.

Khairoutdinov, M. and D. Randall, 2003: Cloud resolving modeling of the ARM summer 1997 IOP: Model formulations, results, uncertainties, and sensitivities. *J. Atmos. Sci.*, **60**, 607–625., doi:10.1175/1520- 0469(2003)060<0607:CRMOTA>2.0.CO;2.

Klein, S. A., et al., 2009: Intercomparison of model simulations of mixed-phase clouds observed during the ARM Mixed-Phase Arctic Cloud Experiment. I: Single-layer cloud. *Q. J. R. Meteorol. Soc.*, **135**, 979– 1002., doi:10.1002/qj.416.

Kolstad, E. W., 2017, Higher ocean wind speeds during marine cold air outbreaks. Q.J.R. Meteorol. Soc., **143,** 2084–2092. doi:10.1002/qj.3068.

Manabe, S. and R. T. Wetherald, 1967: Thermal equilibrium of the atmosphere with a given distribution of relative humidity. *J. Atmos. Sci.*, **24**, 241–259., doi: 10.1175/1520-0469(1967)024<0241:TEOTAW>2.0.CO;2.

Martin, G. M., D. W. Johnson, and A. Spice, 1994: The measurement and parameterization of effec- tive radius of droplets in warm stratocumulus clouds. *J. Atmos. Sci.*, **51**, 1823–1842., doi:10.1175/1520- 0469(1994)051<1823:TMAPOE>2.0.CO;2.

Mlawer, E. J., S. J. Taubman, P. D. Brown, M. J. Iacono, and S. A. Clough, 1997: Radiative transfer for inhomogeneous atmosphere: RRTM, a validated correlated-*k* model for the longwave. *J. Geophys. Res.*, **102**, 16 663–16 682., doi:10.1029/97JD00237.

Morris, V. R., 2005: Total Sky Imager (TSI) handbook. ARM TR-017, doi:Available at http://www.arm.gov/publications/tech reports/handbooks/tsi handbook.pdf.

Morrison, H., J. A. Curry, and V. I. Khvorostyanov, 2005: A new double-moment microphysics parame- terization for application in cloud and climate models. Part I: Description. *J. Atmos. Sci.*, **62**, 1665–1677., doi:10.1175/JAS3446.1.

References

Morrison, H. and J. O. Pinto, 2006: Intercomparison of bulk cloud microphysics schemes in mesoscale simulations of springtime Arctic mixed-phase stratiform clouds. *Mon. Wea. Rev.*, **134**, 1880–1900., doi: 10.1175/MWR3154.1.

Morrison, H., G. Thompson, and V. Tatarskii, 2009: Impact of cloud microphysics on the development of trailing stratiform precipitation in a simulated squall line: Comparison of One- and Two-Moment schemes. *Mon. Wea. Rev.*, **137**, 991–1007., doi:10.1175/2008MWR2556.1.

Myhre, G., et al., 2013: Anthropogenic and natural radiative forcing. *Climate Change 2013: The Physical Science Basis. Contribution of Working Group I to the Fifth Assessment Report of the Intergovernmental Panel on Climate Change*, T. F. Stocker, D. Qin, G.-K. Plattner, M. Tignor, S. K. Allen, J. Boschung, A. Nauels, Y. Xia, V. Bex, and P. M. Midgley (eds.), Cambridge University Press, Cambridge, United Kingdom and New York, NY, USA.

Redelsperger, J. L. and G. Sommeria, 1986: Three-dimensional simulation of a convective storm: Sen- sitivity studies on subgrid parameterization and spatial resolution. *J. Atmos. Sci.*, **43**, 2619–2635., doi: 10.1175/1520-0469(1986)043<2619:TDSOAC>2.0.CO;2.

Reynolds, R. W., 2009: What's new in version 2. Tech. rep., NOAA/NCDC Rep., 10 pp. doi:www.ncdc.noaa.gov/sites/default/files/attachments/Reynolds2009 oisst daily v02r00 version2-features.pdf.

Reynolds, R. W., T. M. Smith, C. Liu, D. B. Chelton, K. S. Casey, and M. G. Schlax, 2007: Daily high-resolution-blended analyses for sea surface temperature. *J. Climate*, **20**, 5473–5496., doi: 10.1175/2007JCLI1824.1.

Stanford, M. W., 2016: Evaluation of simulated tropical convective updraft hydrometeor properties using aircraft observations. *Thesis, Department of Atmospheric Sciences, University of Utah, Salt Lake City.*, 101 pp.

Teixeira, J. and S. Cheinet, 2004: A simple mixing length formulation for the eddy-diffusivity parameteri- zation of dry convection. *Bound.-Layer Meteor.*, **110**, 435–453., doi:10.1023/B:BOUN. 0000007230.96303.0d.

Tompkins, A. M., and A. G. Semie, 2017: Organization of tropical convection in low vertical wind shears: Role of updraft entrainment, J. Adv. Model. Earth Syst., 9, 1046–1068, doi: 10.1002/2016MS000802.

Trenberth K. E., J. T. Fasullo, and J. Kiehl, 2009: Earth's global energy budget. Bull. Amer. Meteor. Soc., **90**, 311—323., doi: 10.1175/2008BAMS2634.1.

Varble, A. C., 2013: Using Tropical Warm Pool-International Cloud Experiment observations to evalu- ate and improve high resolution simulations of tropical convective precipitation systems. *Dissertation, Department of Atmospheric Sciences, University of Utah, Salt Lake City.*, 239 pp.

Widener K, Bharadwaj N, Johnson K, 2012: Ka-band arm zenith radar handbook. ARM Technical report DOE/SC-ARM/TR-106, 19 p

Zelinka, M. D., S. A. Klein, and D. L. Hartmann, 2012a: Computing and partitioning cloud feed- backs using cloud property histograms. Part I: Cloud radiative kernels. *J. Climate*, **25**, 3715–3735., doi: 10.1175/JCLI-D-11-00248.1.

Zelinka, M. D., S. A. Klein, and D. L. Hartmann, 2012b: Computing and partitioning cloud feedbacks using cloud property histograms. Part II: Attribution to changes in cloud amount, altitude, and optical depth. *J. Climate*, **25**, 3736–3754., doi:10.1175/JCLI-D-11-00249.1.

Zhang, M. H. and J. L. Lin, 1997: Constrained variational analysis of sounding data based on column- integrated conservations of mass, heat, moisture, and momentum: Approach and application to ARM measurements. *J. Atmos. Sci.*, **54**, 1503–1524., doi:10.1175/1520-0469(1997)054<1503:CVAOSD>2.0.CO;2.

Zhang, M. H., J. L. Lin, R. T. Cederwall, J. J. Yio, and S. C. Xie, 2001: Objective analy- sis of ARM IOP data: Method and sensitivity. *Mon. Wea. Rev.*, **129**, 295–311., doi:10.1175/1520-0493(2001)129<0295:OAOAID>2.0.CO;2.

Zhou, C., M. D. Zelinka, A. E. Dessler, and P. Yang, 2013: An analysis of the short-term cloud feedback using MODIS data. *J. Climate*, **26**, 4803–4815., doi:10.1175/JCLI-D-12-00547.1.